Spring 1-1-2010

Assessing Habitability of Aqueous Environments on Mars

Lindsey Link Tierney
University of Colorado at Boulder, lindsey.link@colorado.edu

ASSESSING HABITABILITY OF AQUEOUS ENVIRONMENTS ON MARS

by

LINDSEY LINK TIERNEY

B.S., University of Arizona, 2003

A thesis submitted to the

Faculty of the Graduate School of the

University of Colorado in partial fulfillment

of the requirement for the degree of

Master of Science

Department of Geological Sciences

2010

This thesis entitled:

Assessing Habitability of Aqueous Environments on Mars

written by Lindsey Link Tierney

has been approved for the Department of Geological Sciences

_____

Bruce Jakosky, committee chair

_____

Thomas M. McCollom, committee member

_____

Alexis Templeton, committee member

Date: _____

The final copy of this thesis has been examined by the signatories, and we find that both the content and the form meet acceptable presentation standards of scholarly work in the above mentioned discipline.

Tierney, Lindsey Link (M.S., Geological Sciences)

Assessing Habitability of Aqueous Environments on Mars

Thesis directed by Professor Bruce M. Jakosky

A source of metabolic energy is a requirement for life. One possible source of energy that may have supported potential organisms on Mars was geochemical energy from chemical disequilibrium. We evaluated the habitability of aqueous environments on Mars by quantifying the amount of available geochemical energy from chemosynthetic reactions from a range of martian environments. By determining the overall Gibbs energy yields for redox reactions in the H-O-C-S-Fe system, the amount of geochemical energy that was available for potential chemolithoautotrophic microorganisms was quantified and the amount of biomass that could have been sustained was estimated. Biomass estimates show that Fe and S redox reactions in basalt aquifers may have supported the production of 10^{12} cells of biomass per kg of altered basalt. Additionally, a putative martian subsurface hydrothermal system would have had the potential to support a maximum of 10^{9} cells per kilogram of vent fluid. The geochemical models indicate that aqueous environments on Mars would have had the potential to generate chemical energy sources to allow for habitable environments, and potential populations of organisms at subsurface hydrothermal systems on Mars would have been approximately two orders of magnitude less than what was modeled for terrestrial hydrothermal systems. Furthermore, the results were applied to four of the Mars Science Laboratory potential landing sites in order to assess which sites may have had the most biological potential. The most habitable sites are considered here to be Gale Crater and Marwth Vallis based on mineralogical evidence with various oxidation states of Fe and S.

DEDICATION

To my delightful daughter, Ashlyn Jean, my soon-to-be baby boy,

and wonderful husband, Kenneth Tierney

You are my life as I know it!

ACKNOWLEDMENTS

There are many people who have supported this work both professionally and personally. I would first like to thank my advisor, Bruce Jakosky, for his support and guidance. Bruce and I may have not spent many working hours together, but he was always willing to give me sound advice, thoughtful discussions and encouragement. He was extremely understanding with my goal of being not only a great researcher, but also a great mother and wife.

I have so much gratitude towards my husband, Ken, for supporting me emotionally throughout this entire process. And to my daughter, Ashlyn, who made me realize everyday why I was working so hard to complete this project. A huge amount of thanks goes to my parents, David and Roxanne Link, for stimulating my scientific-natured brain even as a child. The last year of research and writing for my thesis may not have been possible if I didn't have my parents love and support for me and for my family.

I also have to thank Dr. Malen Link and Dr. Andrew Redd for showing me that graduate school isn't so scary. Malen, my sister, has been my role model from the very beginning and was a constant source of support and understanding throughout my graduate career.

I would like to also thank my committee members: Tom McCollom and Alexis Templeton. They both contributed to this research in one way or another. Their feedback on my modeling and manuscript drafts was essential.

And to the Boulder graduate students with whom I spent many hours talking about Mars and/or the possibility of life on other planets at various happy hours. My office mates Damhnait Gleeson, Nate Murphy, and Monica Hoke made coming to work fun and stimulating. Lastly, there are numerous friends/colleagues (alphabetically) who supported me and this research in

one way or another; Patricia Badiuk, Nicole Cates, Kristi Dixon, Emily Knowles, Jason Korner, Brittany and Tim Martin, Sarah Martin, Lisa Mayhew, Ruben Rabassa, Sheri Robenstine, Hanna Sizemore, Elizabeth Swanner, and Dustin Trail.

This research was supported by the NASA Astrobiology Institute through a Cooperative Agreement with the University of Colorado.

CONTENTS

TABLES

Table

FIGURES

Figure

CHAPTER 1

INTRODUCTION

"Are they worlds, or are they mere masses of matter? Are physical forces alone at work there or has evolution begotten something more complex, something not unakin to what we know on Earth as life? It is in this that lies the peculiar interest of Mars."

— Percival Lowell, Mars*, 1896*

Life as we know it requires water as well as access to biogenic elements and energy from chemical disequilibrium to drive metabolism. On Mars, liquid water was more abundant in the past and may even be present in the subsurface today. There is morphological evidence for dendritic valley networks [Carr and Clow, 1981; Carr and Malin, 2000; Craddock and Howard, 2002], outflow channels [Baker et al., 1992] and crater lakes [Cabrol et al., 1998; Cabrol and Grin, 1999; Malin and Edgett, 2003] in ancient times that show that water was persistent on the surface. Hydrated minerals have also been detected at the surface from orbiters [Christensen et al., 2000; Poulet et al., 2005; Bibring et al., 2005; Bibring et al., 2006; Mustard et al., 2008; Murchie et al., 2009] and also identified within martian meteorites [Mcsween, 1994; Gooding, 1992; Treiman et al., 2000]. These hydrated minerals most likely formed as alteration products after the interaction with water at high or low temperatures. Gullies have also been identified on relatively young landforms and thus are thought to have formed in more recent epochs on Mars [Malin et al., 2006]. With the abundant evidence for liquid water at or near the surface of Mars over time, water would have been available for potential organisms, but should not be the sole driving force when assessing habitability of an environment on Mars.

Energy is another requirement for life and can also be used to evaluate the habitability of an aqueous system. The more Gibbs energy available, the more biological potential there is for that system. On Earth, the sun provides energy for most living organisms via photosynthesis, but photosynthesis may have never evolved on Mars and was not dominant on development of the earliest life on Earth [e.g. Nisbet and Sleep, 2001]. A possible source of energy for potential martian organisms, however, would have been via chemosynthesis [Shock, 1997; Fisk and Giovannoni, 1999; Jakosky and Shock, 1998]. Chemosynthetic reactions take advantage of the redox (reduction/oxidation) chemical disequilibrium that occurs in aqueous environments. Chemical disequilibrium can occur at low temperatures when there is a contrast in oxidation states between reduced basaltic rocks and relatively oxidized water. In higher-temperature systems, reducing hydrothermal fluids can be out of equilibrium with more oxidizing water. Organisms that take advantage of this chemical disequilibrium, chemolithoautotrophs for example, can exploit the disequilibrium in the environment and in return gain metabolic energy [McCollom and Shock, 1997; McCollom, 2000; Edwards et al., 2005]. Chemolithoautotrophs are organisms that obtain energy from redox reactions involving inorganic compounds and can grow on CO_2 as its only carbon source. The overall Gibbs energy yields of redox reactions that result from chemical disequilibria can be calculated and used to determine the feasibility of various metabolisms in specific environments, and thus can be used as a constraint on habitability.

There are a number of redox reactions that are known on Earth to supply geochemical energy to chemolithoautotrophic organisms (Table 1). These chemosynthetic reactions are known to occur in a variety of environments that include basalt aquifers, hot springs, and subsurface hydrothermal systems. The reactions in Table 1 may have provided sources of

Table 1: Chemolithoautotrophic reactions considered in this study that may have provided energy sources to potential martian organisms.

Rxn #	Involving mainly aqueous species	
1	$H_2S + 2\ O_{2(aq)} = SO_4^{2-} + 2\ H^+$	(Sulfide oxidation)
2	$Pyrite + H_2O + 3.5\ O_{2(aq)} = Fe^{2+} + 2\ SO_4^{2-} + 2\ H^+$	(Pyrite oxidation)
3	$SO_4^{2-} + 2\ H^+ + 4\ H_{2(aq)} = H_2S + 4\ H_2O$	(Sulfate reduction)
4	$Fe^{2+}\ 0.25\ O_{2(aq)} + H^+ = Fe^{3+} + 0.5\ H_2O$	(Iron oxidation)
5	$Fe^{2+} + H_2O + 0.25\ O_{2(aq)} = 0.5\ Hematite + 2\ H^+$	(Iron oxidation-precip)
6	$Fe^{3+} + 0.5\ H_{2(aq)} = Fe^{2+} + H^+$	(Iron reduction)
7	$Goethite + 2\ H^+ + 0.5\ H_{2(aq)} = 2\ H_2O + Fe^{2+}$	(Goethite reduction)
8	$H_{2(aq)} + 0.5\ O_{2(aq)} = H_2O$	(Hydrogen oxidation)
9	$CH_{4(aq)} + 2\ O_{2(aq)} = 2\ H_2O + CO_{2(aq)}$	(Methanotrophy)
10	$CO_{2(aq)} + 4\ H_{2(aq)} = 2\ H_2O + CH_{4(aq)}$	(Methanogenesis)

energy for potential martian organisms when water was more abundant in the past. This study focused on chemolithoautotrophic reactions from the H-O-C-S-Fe system and only redox reactions involving these aqueous species were considered for this study. Solid mineral surfaces were also assumed to be a source of energy for potential organisms that may have lived on or within the surfaces of the rocks as chemolithoautotrophs are able to mediate reactions which directly involve minerals as a source of energy [Shock, 2009]. Furthermore, reactions that produce H_2 were included because H_2 can be produced from iron oxidation reactions and can act as an electron donor for various chemolithotrophic metabolic pathways [Stevens and McKinley, 1995; Stevens and McKinley, 2000; Chapelle et al., 2002].

Previous studies have employed thermodynamic approaches to calculate the amount of geochemical energy that may be available in various environments. For instance, McCollom and Shock [1997] and McCollom [2000] estimated the amount of metabolic energy produced from terrestrial hydrothermal systems; Bach and Edwards [2003] calculated the amount of energy available to support chemolithoautotrophy primary production at ridge flanks; Varnes et al. [2003] estimated the amount of metabolic energy available from martian hydrothermal systems; Jakosky and Shock [1998] and Link et al. [2005] calculated the amount of geochemical energy released from low-temperature weathering reactions on Mars; Jepsen et al. [2007] calculated available energy from shallow water environments on Mars, and McCollom [1999] estimated the amount of metabolic energy available at hydrothermal systems on Europa. Similar to these previous studies, a thermodynamic approach was used in this study to assess the biological potential of Mars at a time when aqueous systems may have been habitable.

To determine the feasibility of these various metabolic pathways, the chemistry of the system must be understood in order to calculate if the reaction is energetically favorable. The

Gibbs energy of formation is used to determine if the reactions are favorable, or can release energy (exergonic). To calculate the change in Gibbs energy in a non-standard state produced from each redox reaction, the following equation was used:

$$\Delta G = \Delta G^{o} + RT\ln Q \qquad (1)$$

where ΔG is the change that occurs during the reaction at specific conditions, $\Delta G°$ is Gibbs energy in a standard state, R is the universal gas constant (8.314 J K^{-1} mol^{-1}), T is the temperature in Kelvin, and Q stands for the activity quotient of the reactants and products based on all of chemical species involved in the fluid for the reaction. The activities of H_2O and minerals were assumed to be 1. The fluid compositions of Mars are largely unknown, but were likely controlled by the interaction with basalt and the atmosphere. The fluid composition determines what the value of "Q" will be. If the overall Gibbs energy of a reaction is exergonic (change in Gibbs energy is negative), then the reaction will give off energy as it proceeds and is favorable for providing energy for microbial metabolism [see McCollom and Shock, 1997].

A thermodynamic reaction path was used to estimate the variations in the compositions of the fluids during mixing. The reaction path was generated by the computer program REACT within Geochemist's Workbench (GWB) 6.0. The reaction path begins by calculating the system's initial equilibrium state. The program then changes the system by adding or titrating reactants to vary the system's composition, changing the temperature or varying the fugacity of gases until all of the reactant has reacted. As the chemical system evolves, the program calculates the abundance and distribution of activities of species in solution, mineral precipitation, and fugacities of gases. This program is used in combination with a

thermodynamic database that contains the properties of aqueous species, minerals, gases, and equilibrium constants for a temperature range of 0-300°C. The database used in this study was "thermo.dat" which is included as a database in GWB and is the most commonly used database for systems with moderate to low ionic strengths, which was the case for all models in this study. This database supports activity coefficients calculated according to an extended form of the Debye-Huckel equation (the "B-dot equation") [Bethke, 1996]. All standard energies (ΔG^o) for the chemolithotrophic reactions were also calculated using GWB from the equilibrium constants in the database listed above.

The goal of this study was to evaluate the habitability of Mars based on the amount of geochemical energy released from numerous redox reactions. Geochemical models were used to calculate fluid compositions that resulted from disequilibrium in aqueous settings, and the amount of available geochemical energy was determined for chemolithoautotrophic reactions. The amount of energy was then used to estimate the amount of biomass that may have been supported. The quantity of biomass that can be formed and supported within a system depends on energy availability, thus sites that have higher levels of energy have greater potential to support life.

The subsequent sections describe each reaction path model and the consequent energy and biomass results. The energy results are then compared to theoretical thermodynamic models performed by others, and the biomass results are compared to analogous terrestrial systems in order to assess the biological potential of martian aqueous systems. Furthermore, we describe each potential landing site for the upcoming Mars Science Laboratory mission and evaluate their biological potential based on energy availability.

CHAPTER 2

REACTION PATH MODELS

Reaction path modeling was used to simulate the chemical evolution of six specific systems and calculate Gibbs energy yields in order to determine which of these hypothetical systems on Mars may have had the most biological potential. All of the systems modeled in this study possessed some type of chemical disequilibrium which may have been used as energy sources for potential organisms.

Six different putative martian environments were modeled that included a range of hypothetical groundwater compositions that reacted with a range of either basaltic host rocks, the atmosphere, or hydrothermal fluids. The resulting fluid compositions from mixing were calculated over the entire reaction path, thus reporting species activities at various water:rock mass ratios and temperature. The six environments were meant to incorporate a range of water and rock compositions, water:rock mass ratios, atmospheric fugacities, pH, and temperatures. Each of these models can be applied to specific sites on Mars including environments similar to Meridiani Planum and Gusev and other sites where liquid water was known or suspected to have been present. Specifically, the mixing models represent environments where near-surface groundwater interacted with basalt (Models 1 and 2); subsurface groundwater interacted with basalt (Model 3); hydrothermal fluid interacted with the atmosphere (Model 4); and hydrothermal fluid mixed with low-temperature groundwater (Models 5 and 6) all of which we present in more detail below. The chemical disequilibrium from basalt aquifers (Models 1, 2 and 3) was assumed to have come from two different sources; 1) the fluid composition from the fluid-rock interaction and 2) the oxidation of reduced minerals in the basalt. The source of

chemical disequilibrium from the hot spring environment (Model 4) came from the fluid composition from the interaction of hydrothermal fluid and atmosphere. The source of the chemical disequilibrium from the subsurface hydrothermal systems (Models 5 and 6) arose in the fluid compositions from the hydrothermal vent fluid-groundwater interactions.

It cannot always be assumed that redox reactions in aqueous systems, especially at low temperatures, approach thermodynamic equilibrium. For all six models, redox reactions in the H-O-C-S-Fe system were decoupled, meaning it was presumed that the rates of the redox reactions were significantly slower than the rates of mixing processes, allowing for the development of redox disequilibrium. Also, all saturated minerals were allowed to precipitate.

2.1 Shallow basalt aquifer (Model 1)

This specific scenario (Model 1) represents an aqueous, shallow environment on Mars that had access to the atmosphere. The chemistry of the near-surface groundwater was controlled by interaction with the atmosphere and the surrounding basalt. This type of basalt-groundwater interaction could have occurred anywhere on Mars where groundwater was in contact with both the atmosphere and basalt, such as a shallow basalt aquifer. This kind of environment is most important for near-future exploration of Mars as the search for evidence of past life will be limited to the near suface. Due to slow reaction kinetics at this low temperature, it was assumed that the basalt and groundwater would have been in a state of disequilibrium.

Initially, pure water was equilibrated with a present-day martian atmosphere at a temperature of 2°C. Present-day compositions of $CO_{2(g)}$, $O_{2(g)}$, $H_{2(g)}$ and $CH_{4(g)}$ were used (log fCO_2 = -2.24, which is equivalent to 6 mbars, log fO_2 = -5, $H_{2(g)}$ = 15 ppm and $CH_{4(g)}$ = 10 ppb). The composition of the resulting, equilibrated groundwater is shown in Table 2. This

Table 2: Activities of hypothetical martian groundwater and hydrothermal fluid compositions. "- -" means values were less than 10^{-12} or not included.

	Groundwater compositions					**Hydrothermal composition**
	Model 1	Model 2	Model 3	Model 5	Model 6	Models 4, 5, and 6
	(Shallow aquifer (pres))	(Shallow aquifer (past))	(Deep aquifer)	(Oxidized)	(Reduced)	(Hydrothermal fluid)
Temp. (°C)	2	2	60	2	60	300
pH	4.96	3.71	6.77	6.86	6.77	6.78
log fO_2	-5.00	-5.00	-10.00	-5.00	-10.00	-33.93
Al^{3+}	--	--	--	6.90E-11	--	--
Ca^{2+}	--	--	8.13E-04	2.52E-03	8.13E-04	5.03E-04
Cl^-	--	--	1.79E-04	1.79E-04	1.79E-04	3.26E-10
$CH_{4(aq)}$	2.13E-11	2.13E-11	1.24E-04	--	1.24E-04	1.38E-06
$\sum CO_{2(aq)}$	4.26E-04	1.35E-01	1.69E-03	1.69E-03	1.69E-03	4.10E-05
Fe^{2+}	--	--	1.59E-07	--	1.59E-07	2.45E-08
Fe^{3+}	--	--	--	--	--	--
K^+	--	--	4.35E-04	1.08E-03	4.35E-04	6.27E-04
$H_{2(aq)}$	1.20E-08	1.20E-08	1.30E-08	--	1.30E-08	4.99E-04
$\sum H_2S_{(aq)}$	--	--	2.12E-06	--	2.12E-06	8.10E-03
Mg^{2+}	--	--	7.63E-04	4.09E-01	7.63E-04	5.37E-06
Mn^{2+}	--	--	7.60E-04	1.99E-11	7.60E-04	1.31E-07
Na^+	--	--	1.65E-03	5.19E-01	1.65E-03	4.91E-01
$SiO_{2(aq)}$	--	--	1.74E-02	1.97E-05	1.74E-02	8.17E-03
SO_4^{2-}	--	--	9.62E-04	5.97E-01	9.62E-04	2.05E-10

groundwater is moderately acidic (pH= 4.96) with trace of amounts of dissolved $H_{2(aq)}$ and $CH_{4(aq)}$. This groundwater composition was then used as the starting composition of the reaction path, and increments of the basalt were then titrated in.

The model simulated a system where basalt (10 kg) was titrated into the groundwater (1 kg) in small increments to produce groundwater:basalt mass ratios of 0.1, 1, 10, and 100 at a fixed temperature of 2°C. The assumed composition of the martian basalt was based on bulk chemical compositions from the martian meteorite Shergotty and were entered into the model as oxides as shown in Table 3. The shergottites represent basalt on Mars that was relatively unaltered and most likely resided near the surface.

After all of the basalt was reacted (groundwater:basalt ratio reached 0.1), the pH rose to 7.19. This is to be expected as the water becomes more mineral dominated. Secondary minerals such as dawsonite, dolomite, magnesite, siderite (carbonates), and kaolinite, muscovite, and nonronite (clays) were predicted to have precipitated in this neutral environment (Table 4). Pyrite and quartz were also predicted to have precipitated. Although carbonates have not been detected on the surface of Mars from orbiters or landers in large abundances, there are spectral signatures that are consistent with Mg-bearing carbonates in the Nili Fossae region [Ehlmann et al., 2008]. Various combinations of carbonates and aluminosilicate clays have been detected in small amounts in the martian meteorites [Gooding, 1992]. Clays, on the other hand, have been detected in various regions of Mars [Bibring et al., 2005; Murchie et al., 2009; Mustard et al., 2008] and are inferred to be products of weathering from more alkaline environments [Poulet et al., 2005; Bibring et al., 2006]. Thus, this model represents a martian environment where near-surface, low-temperature groundwater likely interacted with basalt and the atmosphere and is applicable to a shallow basalt aquifer type of environment.

Table 3: Chemical composition of Shergotty meteorite, Humphrey (RAT 1) basalt, and Gusev soil.

Element	Oxide	Shergotty wt %	Humphrey wt%	Gusev soil wt%
Si	SiO_2	51.36	46.10	45.80
Al	Al_2O_3	7.06	10.90	10.00
Fe	FeO	13.58	14.24	12.64
	Fe_2O_3	5.82	3.56	3.16
Mg	MgO	9.28	10.40	9.30
Ca	CaO	10.00	7.84	6.10
Na	Na_2O	1.29	3.10	3.30
K	K_2O	0.16	0.12	0.41
S	S	0.13	1.02	5.82
P	P_2O_5	0.80	0.60	0.84
Mn	MnO	0.52	0.38	0.31
	total wt	100.00	98.26	97.69

Fe reported as FeO. Shergotty assumed Fe^{3+}/Total Fe = 0.3 [Delaney et al. 1998]; Humphrey (RAT 1) and Gusev soil assumed Fe^{3+}/Total Fe = 0.2 [Gellert et al. 2004].

Table 4: Minerals predicted to precipitate for each model in this study in alphabetical order.

Minerals	Chemical formula	Description	Formed in Model #
Anhydrite	$CaSO_4$	Sulfate	5,6
Antigorite	$Mg_{24}Si_{17}O_{42.5}(OH)_{31}$	Serpentine	5,6
Calcite	$CaCO_3$	Carbonate	3
Dawsonite	$NaAlCO_3(OH)_2$	Carbonate	1,2
Dolomite	$CaMg(CO_3)_2$	Carbonate	1,2,5,6
Gypsum	$CaSO_4{:}2H_2O$	Sulfate	5,6
Kaolinite	$Al_2Si_2O_5(OH)_4$	Clay	1,2
Magnesite	$MgCO_3$	Carbonate	1,2,5,6
Minnesotaite	$Fe_3Si_4O_{10}(OH)_2$	Clay (mica)	3
Muscovite	$KAl_3Si_3O_{10}(OH)_2$	Clay (mica)	1,2
Nontronite	$(Mg/Fe)_2Al_{0.33}Si_{3.67}O_{10}(OH)_2$	Clay (smectite)	1,2,3
Pyrite	FeS_2	Sulfide	1,2,3,4,5,6
Quartz	SiO_2	Silica	1,2,4,5,6
Siderite	$FeCO_3$	Carbonate	1,2
Talc	$Mg_3Si_4O_{10}(OH)_2$	Clay (mica)	5,6

The activities for each species in the H-O-C-Fe-S-system were calculated along the reaction path and are shown in Figure 1. Equation 1 was then used to calculate the resulting Gibbs energies for each reaction in Table 1 using the aqueous activities from Figure 1.

2.1.1 Energy results

The results for Model 1 (Table 5) show that all chemolithotrophic reactions would have been favorable at this type of setting with Gibbs energies ranging from -6 to -1250 kJ/mol Fe, S, C, and H_2 depending on the reaction and the groundwater:basalt ratio. This table includes the Gibbs energies at standard state ($\Delta G°$) and the Gibbs energies (ΔG) averaged over all the water:rock ratios when T=2°C. Aerobic reactions such as methanotrophy, pyrite oxidation and sulfide oxidation would have been the most favorable reactions. Sulfide oxidation for example, (reaction 1, Table 1) releases -755 kJ/mol H_2S at standard conditions ($\Delta G°$). However, the ΔG for this reaction over the entire reaction path was calculated to be between -698 and -714 kJ/mol H_2S as the water:rock ratio was varied (Figure 2a). These values are less than the value at standard state, but are still exergonic and would have been a favorable source of metabolic energy for chemolithotrophic organisms. The figure also shows that the resulting Gibbs energies of sulfide oxidation are not greatly affected by the groundwater:rock ratio. This is also the case for all of the reactions listed in Table 1. The Gibbs energy results for pyrite oxidation and methanotrophy are shown in Figure 2b. Iron oxidation and $H_{2(aq)}$ oxidation are also reactions that would have been favorable for metabolic processes, but would have provided smaller amounts of energy (Figure 2c).

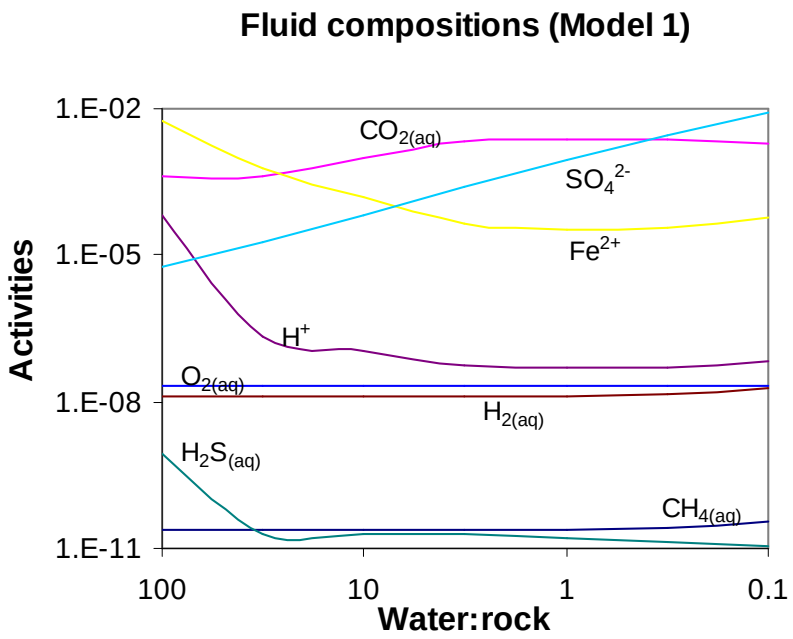

Figure 1: Log-log plot of activities of all relevant species calculated in the H-O-C-S-Fe-system as a result of mixing martian hypothetical groundwater that has been equilibrated with a present martian atmosphere and basalt. $CO_{2(aq)}$ represents the sum of the $CO_{2(aq)}$ and HCO_3^-. $H_2S_{(aq)}$ represents the sum of $H_2S_{(aq)}$ and $HS^-_{(aq)}$. aFe^{3+} ~10^{-20} and not shown on graph.

Table 5: Metabolic energy results and biomass estimates for Model 1 (shallow basalt aquifer (present atmosphere)) when only aqueous components are considered.

Rxn	Equation	ΔG° (kJ/mol S, Fe, H_2, or C)	avg. ΔG (kJ/mol S, Fe, H_2, or C)	LR	ΔG (kJ/kg fluid)	biomass (cells/kg fluid)
1	$H_2S + 2\ O_{2(aq)} = SO_4^{2-} + 2\ H^+$	-755.26	-707.64	H_2S	-9.69E-08	7.75E+02
2	$Pyrite + H_2O + 3.5\ O_{2(aq)} = Fe^{2+} + 2\ SO_4^{2-} + 2\ H^+$	-1252.62	-1238.50	O_2	-7.26E-06	5.81E+04
3	$SO_4^{2-} + 2\ H^+ + 4\ H_{2(aq)} = H_2S_{(aq)} + 4\ H_2O$	-300.81	-101.85	H_2	-3.59E-07	1.03E+04
4	$Fe^{2+}\ 0.25\ O_{2(aq)} + H^+ = Fe^{3+} + 0.5\ H_2O$	-52.23	-87.69	O_2	-7.46E-06	5.97E+04
5	$Fe^{2+} + H_2O + 0.25\ O_{2(aq)} = 0.5\ Hematite + 2\ H^+$	-47.10	-84.29	O_2	-7.16E-06	5.73E+04
6	$Fe^{3+} + 0.5\ H_{2(aq)} = Fe^{2+} + H^+$	-79.78	-13.50	Fe^{3+}	n/a	n/a
7	$Goethite + 2\ H^+ + 0.5\ H_{2(aq)} = 2\ H_2O + Fe^{2+}$	-87.23	-19.21	H_2	-4.50E-07	1.28E+04
8	$H_{2(aq)} + 0.5\ O_{2(aq)} = H_2O$	-263.98	-202.33	H_2	-2.86E-06	3.05E+04
9	$CH_{4(aq)} + 2\ O_{2(aq)} = 2\ H_2O + CO_{2(aq)}$	-859.67	-740.67	CH_4	-1.86E-08	1.49E+02
10	$CO_{2(aq)} + 4\ H_{2(aq)} = 2\ H_2O + CH_{4(aq)}$	-196.19	-68.60	H_2	-2.43E-07	6.94E+03

ΔG° calculated for 2°C. ΔG calculated from Equation 1 (see text) and averaged over all water:rock ratios. LR = limiting reactant. ΔG (kJ/kg fluid) calculated by multiplying the activity of the limiting reactant (Figure 1) at each water:rock ratio by the Gibbs energy and dividing the value if stoichiometry was involved. For biomass calculations, it was assumed that potential aerobes would have required 125 kJ/g biomass and potential anaerobes would have required 35 kJ/g biomass and that only 10% of the energy available is utilized for biomass production. Also, it was assumed that 1 cell weighs 1 x 10^{-13} grams [Phelps et al., 1994]. "n/a" implies negative biomass.

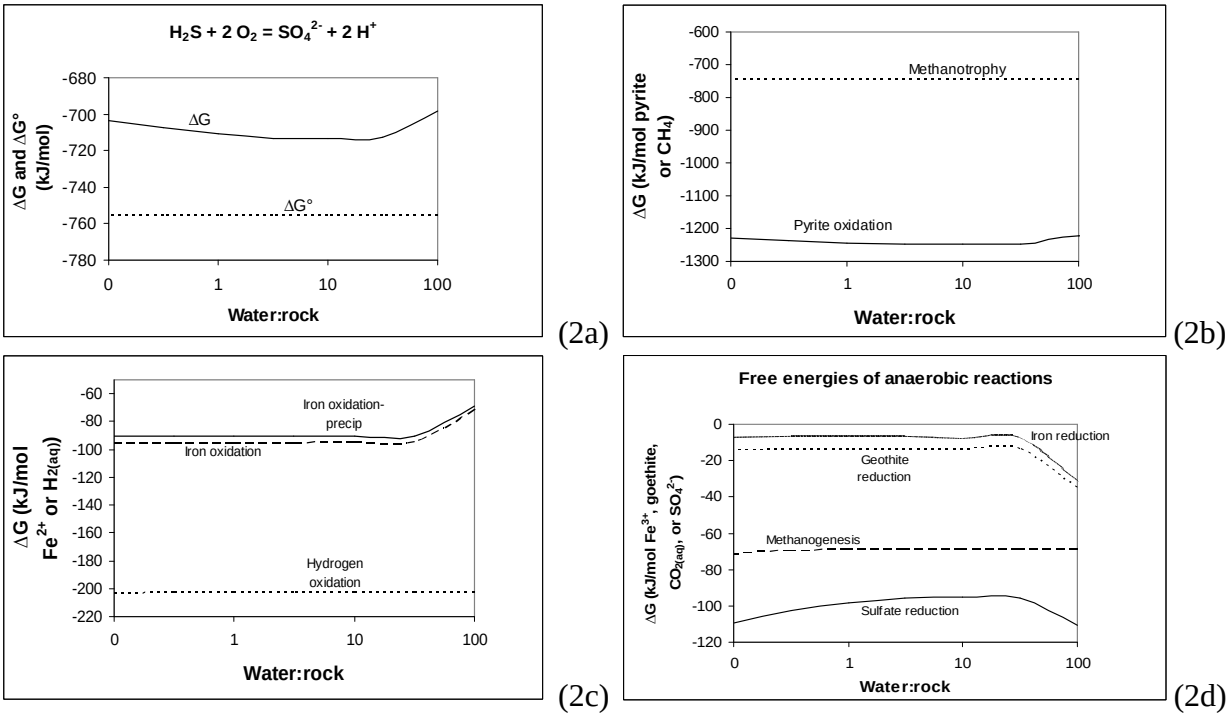

Figure 2: Energy results of chemolithoautotrophic reactions from Table 1 as a function of water:rock ratio as a result of mixing hypothetical martian groundwater and basalt at 2°C (Model 1). (a) $\Delta G°$ and ΔG are shown for sulfide oxidation (Reaction 1) expressed in kJ per mole of H_2S reacted. (b) ΔG of pyrite oxidation (Reaction 2) and methanotrophy (Reaction 9) expressed in terms of kJ per mole of pyrite or CH_4. (c) ΔG of iron oxidation (Reactions 4 and 5) and hydrogen oxidation (Reaction 8) expressed in terms of kJ per mole of Fe^{2+} or $H_{2(aq)}$. (d) ΔG of iron reduction (Reactions 6 and 7), methanogenesis (Reaction 10), and sulfate reduction (Reaction 3) expressed in terms of kJ per mole of Fe^{3+}, SO_4^{2-} or $CO_{2(aq)}$.

The anaerobic reactions (the reactions that do not require O_2) in this study were assumed to use $H_{2(aq)}$ as an electron donor in order to reduce sulfate, ferric iron or CO_2. Reactions that require $H_{2(aq)}$ as an electron donor are also favorable sources of metabolic energy for potential chemolithotrophs even with low concentrations of $H_{2(aq)}$ on the order of 10^{-8} molal. Present atmospheric compositions report ~15ppm of $H_{2(g)}$ in the atmosphere [Krasnopolsky and Feldman, 2001]. If the groundwater was in equilibrium with the atmosphere, then the atmosphere would have been a constant source for $H_{2(aq)}$ in near-surface groundwater. This is also the case for $CH_{4(g)}$ which was detected in the ppb levels in the martian atmosphere [Formisano et al., 2004]. The Gibbs energies for sulfate, ferric iron, goethite, and CO_2 reduction (methanogenesis) are all shown in Figure 2d. It can be seen that all reactions are exergonic, but lesser amounts of energy would have been available for potential martian organisms.

These reported Gibbs energy values represent how thermodynamically favorable a reaction might have been. Although all of the reactions for this model are favorable, the extent of the reaction progress depends on the availability of each reactant. For instance, sulfide oxidation (reaction 1) requires H_2S and $O_{2(aq)}$ for the reaction to proceed. Figure 1 shows that H_2S activities are less than $O_{2(aq)}$ at all water:rock ratios. This implies that H_2S was likely to be the limiting factor for this metabolism. It is more useful then to take into account the activities and stoichiometry of each reaction in order to express the Gibbs energies in terms of units of energy per the one kilogram of fluid used[McCollom and Shock, 1997; McCollom, 1999]. The Gibbs energies were calculated by multiplying the activity of the limiting reactant at each water:rock ratio by the Gibbs energy and dividing the value if stoichiometry was involved. This Gibbs energy value is now expressed in terms of kJ per kilogram of fluid with H_2S being the limiting factor and is shown in Table 5. For example, the average Gibbs energy for sulfide

oxidation would have been -9.69 x 10^{-8} kJ/kg of fluid. This value is low and shows that the limiting reactant plays an important role when expressing Gibbs energies. Table 5 also demonstrates that potential chemolithotrophic organisms that would have taken advantage of redox reactions that involved mainly aqueous species and were living in shallow basalt aquifers could not have relied on significant amounts of Gibbs energy for metabolism. Instead, if the amount of limiting reactant was somehow increased, possibly from an outside source not considered in our model, then more Gibbs energy would have been available per the kg of fluid, and thus there would have been more biological potential. An additional volcanic source that may have supplied added H_2S (for Reaction 1), or hydrolysis of ferrous iron to produce increased amounts of $H_{2(aq)}$ (for Reactions 3, 7, 8, and 10) are plausible potential ways to increase concentrations of the limiting reactants.

2.1.2 Biomass estimates

The amounts of available Gibbs energy for each reaction can be converted to biomass production if we assume that autotrophic aerobes require 80-170 kJ to produce 1 gram dry weight of biomass, and autotrophic anaerobes require 30-40 kJ/g biomass [Heijnen and van Dijken, 1992]. For this study, we assumed that potential aerobes would have required 125 kJ/g biomass and potential anaerobes would have required 35 kJ/g biomass and that only 10% of the energy available is utilized for biomass production. However, it has been suggested that organisms in actively growing cultures require 20 kJ/mol to drive ATP synthesis [Schink, 1997] and that starving populations may only require 12 to 15 kJ/mol [Schink and Stams, 2002]. Sulfide oxidation, again as an example, can produce 0.57 grams dry weight biomass for every mole of H_2S or 7.75 x 10^{-11} grams per kg fluid which is equivalent to 77 g/km^3 fluid.

2.1.3 Solid-mineral components

Additional chemical energy can potentially be derived from redox reactions involving solid-mineral components such as iron and sulfur minerals present in the basalt. However, the energy metabolism of a solid requires specialized electron transfer machinery such as excreted chelating agents or membrane-bound electron transfer proteins [Hernandez, 2001]. Nevertheless, terrestrial organisms have been discovered that are able to use minerals as energy sources [Shock, 2009]. In order to calculate the amount of geochemical energy that would have been available to support microbial biomass production from metabolism of the solid component, the extent of iron and sulfur oxidation needed to be determined for martian basalt. The principle behind this approach is outlined in Bach and Edwards [2003]. To determine the degree of iron oxidation of the martian basalt, the average primary iron content and oxidation state of iron in pristine basalt was required. Table 3 shows the values for Shergotty meteorite that was used for this model. Total Fe in Shergotty is reported to be 19.40 wt % with the oxidation state reported as Fe^{3+}/total Fe = 0.3 [Delaney et al., 1998]. Using an average total Fe content of 19.40 wt % and a pre-alteration oxidation state of 0.3, the ferrous Fe content was therefore estimated to be 13.58 wt %. Altered martian basalt values of Fe^{3+}/total Fe can range from 0.6-0.9 for pervasively altered rock analyzed from the Gusev site [Morris et al., 2006], for example. We here assumed an average Fe oxidation state of Fe^{3+}/total Fe = 0.75 which is an increase of Fe^{3+}/total Fe = 0.45. The degree of Fe oxidation is thus calculated to have been 8.73 wt% Fe that would have been oxidized. This equates to 87.3 g Fe/kg basalt that was oxidized (1.56 mol Fe/kg basalt).

The pre-alteration concentration of sulfur was determined by the following empirical formula discussed in Bach and Edwards [2003] based on the amount of Fe for sulfide-saturated basalts [Mathez, 1979].

$$S\ [wt\%] = 0.023\ Fe\ [wt\%] - 0.059 \quad (2)$$

The sulfur concentration corresponding to a Shergotty host rock Fe content of 19.41 wt% is 0.387 wt% S. As Bach and Edwards [2003] explain, S is lost through oxidation of primary metal sulfides and terrestrial values can range from ~50-90% loss of S. We assume a sulfur loss to oxidation of 90% because of the lack of evidence for iron sulfides on Mars, and estimated that average altered martian basalt has lost 0.348 wt% S (0.11 mol S/kg basalt).

The production of $H_{2(g)}$ has been suggested to form from the oxidation of Fe-bearing mineral phases with low-temperature water [Stevens and McKinley, 1995; Stevens and McKinley, 2000; Chapelle et al., 2002] with an example reaction shown below.

$$2FeO + H_2O = Fe_2O_3 + H_2 \quad (3)$$

Again, as discussed by Bach and Edwards [2003], we assume that ~50% of the oxidation of iron is from hydrolysis reactions like the one shown above. This now translates to 0.78 mol Fe/kg basalt that was oxidized by hydrolysis and thus 0.39 mol H_2 can be produced for every 1 kg of basalt.

2.1.3.1 Energy calculations and biomass estimates

The Fe and S oxidation estimates along with H_2 production were used to calculate the amount of geochemical energy available to support chemolithoautotrophic metabolisms. Results of the biomass calculations are presented in Table 6. The total amount of biomass that could have been produced by Fe-oxidizers would have been 54 mg/kg basalt and 30mg/kg basalt for Fe-reducers. The total amount of biomass that could have been produced by S-oxidizes would have been 62 mg/kg basalt and 28 mg/kg basalt for S-reducers. H_2-consuming reactions could have produced 19 mg/kg basalt from methanogenesis and 225 mg/kg basalt from hydrogen oxidation.

2.2 Factoring in additional CO_2 (Model 2)

There is a great amount of evidence that shows that early Mars may have had greater levels of $CO_{2(g)}$ than what is seen today based on atmospheric models and morphology. For this reason, Model 1 was recalculated with an assumed higher abundance of $CO_{2(g)}$ in the atmosphere and will be referred to as Model 2. All other assumptions and calculations were carried out in the same manner as Model 1. In order to explain the stability of liquid water at the surface for prolonged time periods, a greenhouse gas such as CO_2 would have been needed to raise the surface temperature of Mars enough to allow liquid water. Several bars of $CO_{2(g)}$ are thought to be required to raise the temperature to the melting point of ice [e.g., Kasting, 1991], thus log fCO_2 = .278 (equivalent to 2 bars) was assumed as a representative value, and this value was fixed for the entire reaction path. In this case, with the greater amount of $CO_{2(g)}$ in contact with the water, the initial pH of the groundwater would have been more acidic at 3.71 (Table 2). As the same composition of basalt was titrated in at various amounts, the pH rose to 6.18. This environment is slightly more acidic than the previous environment that represented present-day

Table 6: Metabolic energy results and biomass estimates from solid-mineral components for Model 1 (shallow basalt aquifer, present atmosphere), Model 2 (shallow basalt aquifer, past atmosphere) and Model 3 (deep aquifer).

Equation		Model 1			Model 2				Model 3		
	ΔG° (kJ/rxn) 2°C	ΔG (kJ/mol Fe, S, H2)	Energy (kJ/kg basalt)	Biomass (mg/kg basalt)	ΔG (kJ/mol Fe, S, H2)	Energy (kJ/kg basalt)	Biomass (mg/kg basalt)	ΔG° (kJ/rxn) 60°C	ΔG (kJ/mol Fe, S, H2)	Energy (kJ/kg basalt)	Biomass (mg/kg basalt)
$H_2S + 2\ O_{2(aq)} = SO_4^{2-} + 2\ H^+$	-755.26	-707.64	-77.84	62.27	-704.75	-77.52	62.02	-736.71	-667.13	-73.38	58.71
$Pyrite + H_2O + 3.5\ O_{2(aq)} = Fe^{2+} + 2\ SO_4^{2-} + 2\ H^+$	-1252.62	-1238.50	-136.23	108.99	-1233.45	-135.68	108.54	-1217.72	-1145.46	-126.00	100.80
$SO_4^{2-} + 2\ H^+ + 4\ H_{2(aq)} = H_2S_{(aq)} + 4\ H_2O$	-300.81	-25.46	-9.93	28.37	-26.11	-10.18	29.09	-308.11	-3.10	-1.21	3.45
$Fe^{2+}\ 0.25\ O_{2(aq)} + H^+ = Fe^{3+} + 0.5\ H_2O$	-52.23	-87.69	-68.40	54.72	-80.31	-62.64	50.12	-42.68	-86.72	-67.65	54.12
$Fe^{2+} + H_2O + 0.25\ O_{2(aq)} = 0.5\ Hematite + 2\ H^+$	-47.10	-84.29	-65.75	52.60	-77.16	-60.19	48.15	-49.98	-75.54	-58.92	47.13
$Fe^{3+} + 0.5\ H_{2(aq)} = Fe^{2+} + H^+$	-79.78	-27.00	-10.53	30.08	-41.68	-16.25	46.44	-87.93	3.56	1.39	n/a
$Goethite + 2\ H^+ + 0.5\ H_{2(aq)} = 2\ H_2O + Fe^{2+}$	-87.23	-38.43	-7.49	21.41	-52.60	-20.52	58.62	-84.03	-25.63	-10.00	28.56
$H_{2(aq)} + 0.5\ O_{2(aq)} = H_2O$	-263.98	-202.33	-78.91	225.46	-202.25	-78.88	225.37	-261.15	-169.83	-66.23	189.24
$CH_{4(aq)} + 2\ O_{2(aq)} = 2\ H_2O + CO_{2(aq)}$	-859.67	n/a	n/a	n/a	n/a	n/a	n/a	-855.67	n/a	n/	n/a
$CO_{2(aq)} + 4\ H_{2(aq)} = 2\ H_2O + CH_{4(aq)}$	-196.19	-17.15	-6.69	19.11	-20.40	-7.96	22.73	-188.85	5.99	2.34	n/a

ΔG for Models 1 and 2 were calculated from Equation 1 at 2°C with activities from Figures 1 and 3. Model 3 assumed T = 60°C and ΔG was calculated from Equation 1 with activities from Figure 5. Energy in terms of kJ/kg basalt was calculated by multiplying the oxidation estimates of Fe and S or the amount of H_2 production (mol/kg basalt) (see text) by ΔG (kJ/mol Fe, S, or H_2). For biomass calculations, it was assumed that potential aerobes would have required 125 kJ/g biomass and potential anaerobes would have required 35 kJ/g biomass and that only 10% of the energy available is utilized for biomass production. Methanotrophy shows n/a because CH_4 production was not evaluated in this study. n/a also implies negative biomass.

CO_2 concentrations. The resulting mineralogy is also similar to what was reported for Model 1 (Table 4). The species activities for this system are shown in Figure 3.

2.2.1 Energy and biomass estimates

The Gibbs energy calculations show that all chemolithotrophic reactions would have been favorable at this type of environment with Gibbs energies ranging from -20 to -1245 kJ/mol Fe, S, C, and H_2 depending on the reaction and the groundwater:basalt ratio (Table 7 and Figure 4a-b). After factoring in the concentrations of each limiting reactant, the energy availability per kg of fluid drops significantly, thus biomass estimates are low (Table 7) similar to Model 1. The similarities between Model 1 and Model 2 show that the amount of $CO_{2(g)}$ in the atmosphere has little effect on biological potential and that these models are not that sensitive to CO_2 fugacity. In the case of a warmer, wetter Mars (Model 2), overall there was slightly more energy available from all chemolithotrophic reactions calculated for this study (see Figures 4a-b), thus slightly more biological potential.

The Fe and S oxidation estimates along with H_2 production that were calculated for Model 1 were used to calculate the amount of geochemical energy available to support chemolithoautotrophic metabolisms for this model as well. Results of the biomass calculations are presented in Table 6. The total amount of biomass that could have been produced by Fe-oxidizes would have been 50 mg/kg basalt and 46mg/kg basalt for Fe-reducers. The total amount of biomass that could have been produced by S-oxidizers would have been 62 mg/kg basalt and 29 mg/kg basalt for S-reducers. H_2-consuming reactions could have produced 23 mg/kg basalt from methanogenesis and 225 mg/kg basalt from hydrogen oxidation. Again, these results are essentially the same as Model 1.

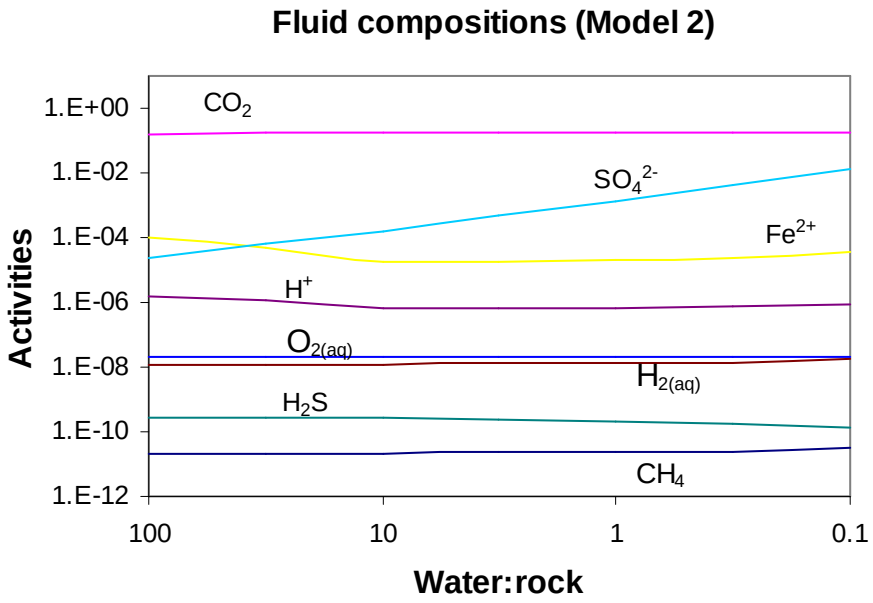

Figure 3: Log-log plot of activities of all relevant species calculated in the H-O-C-S-Fe-system as a result of mixing martian hypothetical groundwater that has been equilibrated with a past martian atmosphere and basalt. $CO_{2(aq)}$ represents the sum of the $CO_{2(aq)}$ and HCO_3^-. $H_2S_{(aq)}$ represents the sum of $H_2S_{(aq)}$ and $HS^-_{(aq)}$. $a\mathrm{Fe}^{3+} \sim 10^{-19}$ and not shown on graph.

Table 7: Metabolic energy results and biomass estimates for Model 2 (Shallow basalt aquifer (past atmosphere)) when only aqueous species are considered.

Rxn	Equation	ΔG° (kJ/mol S, Fe, H_2, or C)	avg. ΔG (kJ/mol S, Fe, H_2, or C)	LR	ΔG (kJ/kg mixed fluid)	biomass (cells/kg mixed fluid)
1	$H_2S + 2\ O_{2(aq)} = SO_4^{2-} + 2\ H^+$	-755.26	-704.75	H_2S	-1.60E-07	1.28E+03
2	$Pyrite + H_2O + 3.5\ O_{2(aq)} = Fe^{2+} + 2\ SO_4^{2-} + 2\ H^+$	-1252.62	-1233.45	O_2	-7.22E-06	5.78E+04
3	$SO_4^{2-} + 2\ H^+ + 4\ H_{2(aq)} = H_2S_{(aq)} + 4\ H_2O$	-300.81	-104.42	H_2	-3.57E-07	1.02E+04
4	$Fe^{2+}\ 0.25\ O_{2(aq)} + H^+ = Fe^{3+} + 0.5\ H_2O$	-52.23	-80.31	O_2	-6.58E-06	5.27E+04
5	$Fe^{2+} + H_2O + 0.25\ O_{2(aq)} = 0.5\ Hematite + 2\ H^+$	-47.10	-77.16	O_2	-6.32E-06	5.06E+04
6	$Fe^{3+} + 0.5\ H_{2(aq)} = Fe^{2+} + H^+$	-79.78	-20.84	Fe^{3+}	n/a	n/a
7	$Goethite + 2\ H^+ + 0.5\ H_{2(aq)} = 2\ H_2O + Fe^{2+}$	-87.23	-26.30	H_2	-7.13E-07	2.04E+04
8	$H_{2(aq)} + 0.5\ O_{2(aq)} = H_2O$	-263.98	-202.25	H_2	-2.74E-06	7.82E+04
9	$CH_{4(aq)} + 2\ O_{2(aq)} = 2\ H_2O + CO_{2(aq)}$	-859.67	-727.35	CH_4	-1.75E-08	1.40E+02
10	$CO_{2(aq)} + 4\ H_{2(aq)} = 2\ H_2O + CH_{4(aq)}$	-196.19	-81.68	H_2	-2.77E-07	7.91E+03

ΔG° calculated for 2°C. Average ΔG calculated from Equation 1 (see text) and averaged over all water:rock ratios. LR = limiting reactant. ΔG (kJ/kg mixed fluid) calculated by multiplying the activity of the limiting reactant (Figure 1) at each water:rock ratio by the Gibbs energy and dividing the value if stoichiometry was involved. For biomass calculations, it was assumed that potential aerobes would have required 125 kJ/g biomass and potential anaerobes would have required 35 kJ/g biomass and that only 10% of the energy available is utilized for biomass production. Also, it was assumed that 1 cell weighs 1 x 10^{-13} grams [Phelps et al., 1994]. "n/a" implies negative biomass.

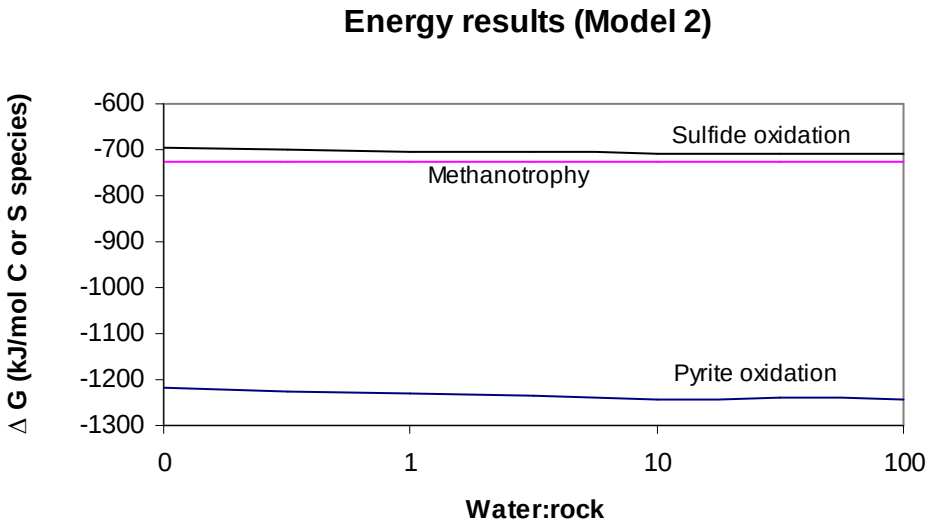

(4a)

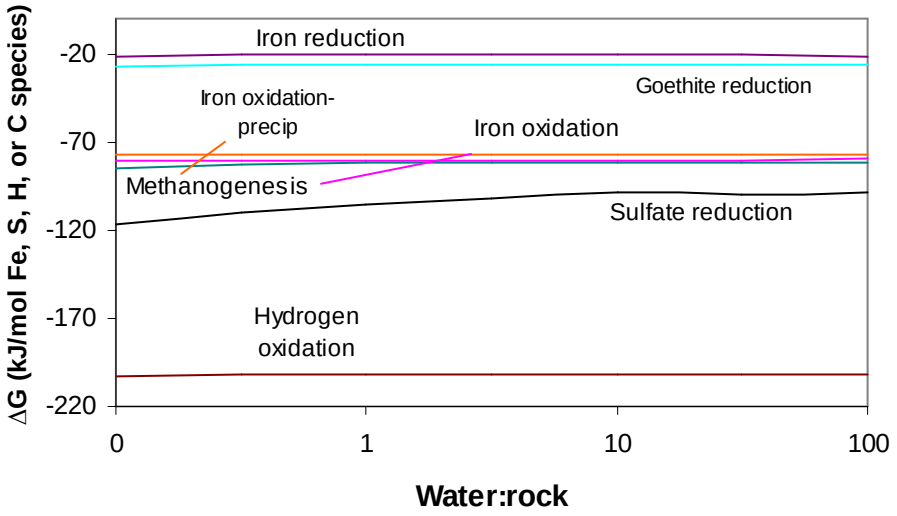

(4b)

Figure 4: Energy results of chemolithoautotrophic reactions from Table 1 as a function of water:rock ratio as a result of mixing hypothetical martian groundwater and basalt at 2°C (Model 2). (a) ΔG is shown for sulfide and pyrite oxidation (Reactions 1 and 2), and methanotrophy (Reaction 9). (b) ΔG is shown for sulfate reduction (Reaction 3), iron oxidation (Reactions 4 and 5), iron and goethite reduction (Reactions 6 and 7), hydrogen oxidation (Reaction 8), and methanogenesis (Reaction 10).

2.3 Deep basalt aquifer (Model 3)

The subsurface of Mars is thought to have been an environment where both liquid water and energy sources would have been available to a potential microbial ecosystem [Fisk and Giovannoni, 1999; Boston et al., 1992]. Both shallow and deep subsurface aquifers are known to flourish with life on Earth. On Mars, subsurface water can express itself as gullies, and there is evidence that exists for this in Mars' recent past and subsurface aquifers may even exist today [Malin and Edgett, 2000]. Thus, it is not only important to model near-surface groundwater with basalt, but it was also important to model the interaction of subsurface groundwater with basalt (Model 3). The groundwater for Model 3 was expected to be more reducing than the near-surface groundwater with less electron acceptors available ($O_{2(aq)}$) and thus provided an environment with relatively reducing conditions as an endmember for groundwater compositions.

The composition of the hypothetical martian subsurface groundwater is highly unknown but was assumed to be similar to subsurface terrestrial groundwater. For this reason, the chemical composition of the groundwater used in this model was assumed to be similar to the chemical composition of groundwater from Lidy Hot Springs [Chapelle et al., 2002] which is found ~200 m below land surface. The Lidy Springs groundwater was thought to be a suitable analog for a subsurface environment on Mars because it was hot (58.5°C), anoxic, lacked organic carbon and had a source of geologically produced hydrogen [Chapelle et al., 2002]. Chapelle et al. [2002] report that the underlying rocks at Lidy Hot Springs are volcanic in origin, and there is a well developed system of geothermal springs that tap deep fault zones. Interestingly, a large number of methanogens were found living in this subsurface environment.

For our model, oxygen fugacity was assumed to be relatively low and a value of logfO_2 = -10 was assumed so that $O_{2(aq)}$ would not be a dominant electron acceptor. The assumed starting composition for this groundwater is shown in Table 2 and is based on values reported in Chapelle et al. [2002]. In these types of environments, an electron donor such as $H_{2(aq)}$ and other reduced compounds are expected to be present from the basalt-groundwater interaction [Stevens and McKinley, 1995], and the electron acceptor may be $CO_{2(aq)}$ or SO_4^{2-} instead of $O_{2(aq)}$ thus providing anaerobic metabolic pathways for potential organisms. Methanogenesis, specifically, is thought to be a dominant metabolic pathway for organisms in the subsurface of Mars or Europa [McCollom, 1999; Boston et al., 1992].

To model this type of martian environment, an unaltered basalt was reacted with a relatively reducing subsurface groundwater. Again, 10 kg of basalt (see Table 3 for Shergotty composition) was titrated into 1 kg of the relatively reducing groundwater and resulting activities were calculated at various water:groundwater ratios (Figure 5). The temperature was fixed at 60°C for the entire reaction path, and minerals were allowed to precipitate. Minerals such as minnesotaite (clay), nontronite (smectite), pyrite (sulfide), and calcite (carbonate) were all predicted to precipitate (Table 4).

2.3.1 Energy and biomass estimates

Equation 1 was used to calculate the Gibbs energy for each reaction listed in Table 1 and the results show that there are a number of reactions that would have been thermodynamically favorable (Table 8). The energies, however, are not as great (not as negative in value) as the previous models. This is expected because there should be less chemical disequilibrium with reduced groundwater and reduced basalt than with an environment that has oxidized groundwater

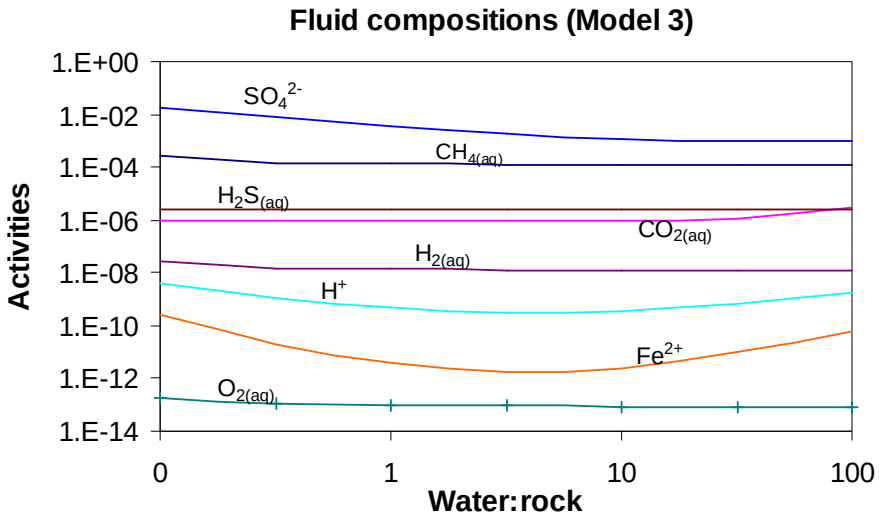

Figure 5: Log-log plot of activities of all relevant species calculated in the H-O-C-S-Fe-system as a result of mixing martian hypothetical subsurface groundwater and basalt (Model 3). $CO_{2(aq)}$ represents the sum of the $CO_{2(aq)}$ and HCO_3^-. $H_2S_{(aq)}$ represents the sum of $H_2S_{(aq)}$ and $HS^-_{(aq)}$. $a Fe^{3+} \sim 10^{-30}$ and not shown on graph.

Table 8: Metabolic energy results and biomass estimates for Model 3.

Rxn	Equation	ΔG° (kJ/mol S, Fe, H_2, or C)	avg. ΔG (kJ/mol S, Fe, H_2, or C)	LR	ΔG (kJ/kg mixed fluid)	biomass (cells/kg mixed fluid)
1	$H_2S + 2\ O_{2(aq)} = SO_4^{2-} + 2\ H^+$	-736.71	-667.13	O2	-3.44E-11	n/a
2	Pyrite + $H_2O + 3.5\ O_{2(aq)} = Fe^{2+} + 2\ SO_4^{2-} + 2\ H^+$	-1217.72	-1145.46	O2	-3.38E-11	n/a
3	$SO_4^{2-} + 2\ H^+ + 4\ H_{2(aq)} = H_2S_{(aq)} + 4\ H_2O$	-308.11	-12.38	H2	-5.76E-08	1.65E+03
4	$Fe^{2+}\ 0.25\ O_{2(aq)} + H^+ = Fe^{3+} + 0.5\ H_2O$	-42.67	-86.72	O2	-3.59E-11	n/a
5	$Fe^{2+} + H_2O + 0.25\ O_{2(aq)} = 0.5$ Hematite $+ 2\ H^+$	-49.97	-75.53	O2	-3.13E-11	n/a
6	$Fe^{3+} + 0.5\ H_{2(aq)} = Fe^{2+} + H^+$	-87.92	1.77	Fe^{3+}	n/a	n/a
7	Goethite $+ 2\ H^+ + 0.5\ H_{2(aq)} = 2\ H_2O + Fe^{2+}$	-84.03	-12.81	H2	-3.99E-07	1.14E+04
8	$H_{2(aq)} + 0.5\ O_{2(aq)} = H_2O$	-261.15	-169.83	O2	-3.52E-11	1.01E+00
9	$CH_{4(aq)} + 2\ O_{2(aq)} = 2\ H_2O + CO_{2(aq)}$	-855.66	-703.17	O2	-3.64E-11	n/a
10	$CO_{2(aq)} + 4\ H_{2(aq)} = 2\ H_2O + CH_{4(aq)}$	-188.85	23.94	H2	n/a	n/a

ΔG° calculated for 60°C. Average ΔG calculated from Equation 1 (see text) and averaged over all water:rock ratios. LR = limiting reactant. ΔG (kJ/kg mixed fluid) calculated by multiplying the activity of the limiting reactant (Figure 1) at each water:rock ratio by the Gibbs energy and dividing the value if stoichiometry was involved. For biomass calculations, it was assumed that potential aerobes would have required 125 kJ/g biomass and potential anaerobes would have required 35 kJ/g biomass and that only 10% of the energy available is utilized for biomass production. Also, it was assumed that 1 cell weighs 1 x 10^{-13} grams [Phelps et al., 1994]. "n/a" implies either negative biomass or less than one cell/kg mixed fluid. Values less than 10^{-12} kJ/kg mixed fluid are not reported.

interacting with reduced basalt. Iron reduction and methanogenesis are, however, not even thermodynamically favorable at the assumed conditions. This is puzzling as Chapelle et al. [2002] found large numbers of methanogens and this reaction is not even favorable for the fluid composition reported in their paper. Furthermore, even though the oxygen level is low, reactions such as sulfide, pyrite, hydrogen, and methane oxidation would still have been energetically favorable (See Table 8). Subsurface aquifers are capable of replenishing H_2 concentrations abiotically by dissolving the basalt with water and producing H_2. H_2 is a very useful electron donor for the reduction of many elements. If the concentration of the electron donor was increased from13 nmol to13μm, then a reaction like methanogenesis would have been favorable and would have had the potential to support 1.67×10^6 cells/kg fluid.

In terms of the amount of available substrate, the anaerobic reactions prove to be the most biologically useful reactions. Sulfate reduction, for instance, would have produced an average of -12.39 kJ per mole sulfate over the range of water:rock ratios. $H_{2(aq)}$, in this case, would have been the limiting reactant, and multiplying the Gibbs energy values by the activities of $H_{2(aq)}$ at each water:rock ratio and dividing by 4 for stoichiometric considerations shows that this value expressed in terms of kg fluid is only -5.76×10^{-8} kJ per kg of fluid averaged over all water:rock ratios. This equates to 1.65×10^{-10} g biomass per kg fluid or 1645 cells per kg fluid.

The Fe and S oxidation estimates along with H_2 production from the solid components of this system were used to calculate the amount of geochemical energy available to support chemolithoautotrophic metabolisms. Results of the biomass calculations are presented in Table 6. The total amount of biomass that could have been produced by Fe-oxidizers would have been 54 mg/kg basalt and 28 mg/kg basalt for Fe-reducers. The total amount of biomass that could have been produced by S-oxidizers would have been 100 mg/kg basalt and 3.5 mg/kg basalt for

S-reducers. H_2-consuming reactions could have supported 189 mg biomass/kg basalt from the hydrogen oxidation reaction.

2.4 Yellowstone on Mars (Model 4)

Surface discharge of hydrothermal fluids on Mars was probably common in the past. Subsurface water would have been heated from either volcanic sources or impacts and would have risen buoyantly and eventually extruded onto the surface. Evidence for this type of model on Mars may exist at Gusev Crater, which includes a deposit with a high abundance of silica. The silica is thought to have formed as a precipitate as hydrothermal water rose, cooled, and gave off dissolved gases [Squyres et al., 2008]. The disequilibrium between the hot, reduced hydrothermal water and the relatively oxidizing atmosphere could have been an environment where potential organisms were able to drive metabolic reactions towards equilibrium and in return gain energy. This type of scenario would have been similar to what we see at Yellowstone, for example. Yellowstone contains hydrothermal water that is heated from a volcanic source and discharges at the surface either as geysers, hot springs or fumaroles. There are numerous examples of microorganisms that thrive in these types of systems and survive by driving chemical reactions towards disequilibrium.

The composition of the martian hydrothermal fluid was determined by modeling the reaction of Humphrey host rock (Table 3) with a dilute groundwater at 300°C. In this case, the basaltic composition was assumed to be from the rock called "Humphrey" found in the unweathered Gusev plains [Gellert et al., 2004; Clark et al., 2005]. The hydrothermal fluid composition is shown in Table 2. As expected, the hypothetical martian hydrothermal fluid would have been reducing ($\log fO_2 = -34.27$ with high quantities of $CH_{4(aq)}$, $H_{2(aq)}$, and H_2S). The

hydrothermal fluid was then modeled to rise towards the surface, cool and interact with a present-day martian atmosphere at 2°C. A temperature v. oxygen fugacity profile is shown in Figure 6.

The reduced hydrothermal fluid would have been in disequilibrium with the relatively oxidizing atmosphere. Based on kinetic inhibitions, redox disequilibrium was allowed and minerals were allowed to precipitate (Table 4). Quartz was predicted to precipitate along the entire reaction path with abundances as high as 0.41 g/kg hydrothermal fluid. Pyrite was also predicted to form, but a much lower abundances (9.8×10^{-8} g/kg fluid). This high abundance of quartz predicted from our model may be applicable to the high concentration of silica detected at Home Plate [Squyres et al., 2008].

2.4.1 Energy and biomass results

The resulting aqueous activities as a function of oxygen fugacity are shown in Figure 7. From these results, the energy yields for each reaction listed in Table 1 were calculated using Equation 1. Figure 8 shows Gibbs energy results for reactions that would have been thermodynamically favorable as a function of $\log fO_2$ and, equivalently, temperature. Pyrite oxidation, sulfide oxidation and methanotrophy are all extremely favorable reactions. All the reactions become more favorable as oxygen fugacity is increased, or in other words, as the fluid reaches the surface. To account for the limiting reactants of each reaction, it may be more reasonable to express these energies based on the concentration of the limiting reactant instead [McCollom and Shock, 1997]. The values in Figure 8 were divided by the stoichiometric coefficient and multiplied by the concentrations of the limiting reactant of the hydrothermal fluid at each temperature in order to calculate the energy available per kg of hydrothermal fluid.

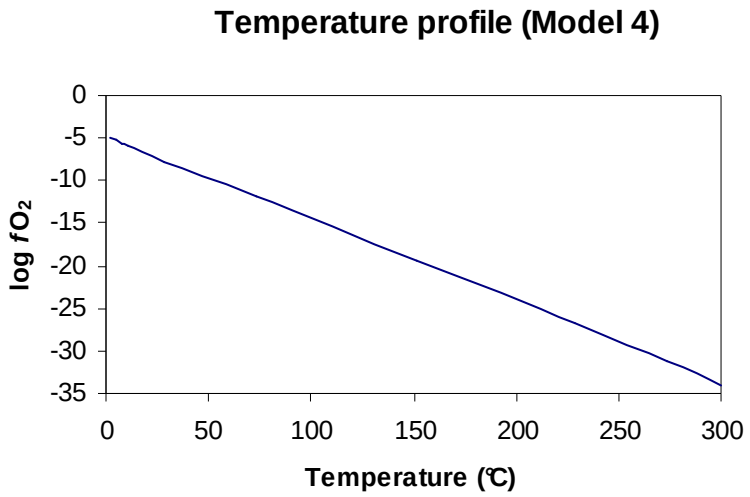

Figure 6: Oxygen fugacity as a function of temperature during mixing hydrothermal fluid and present-day martian atmosphere.

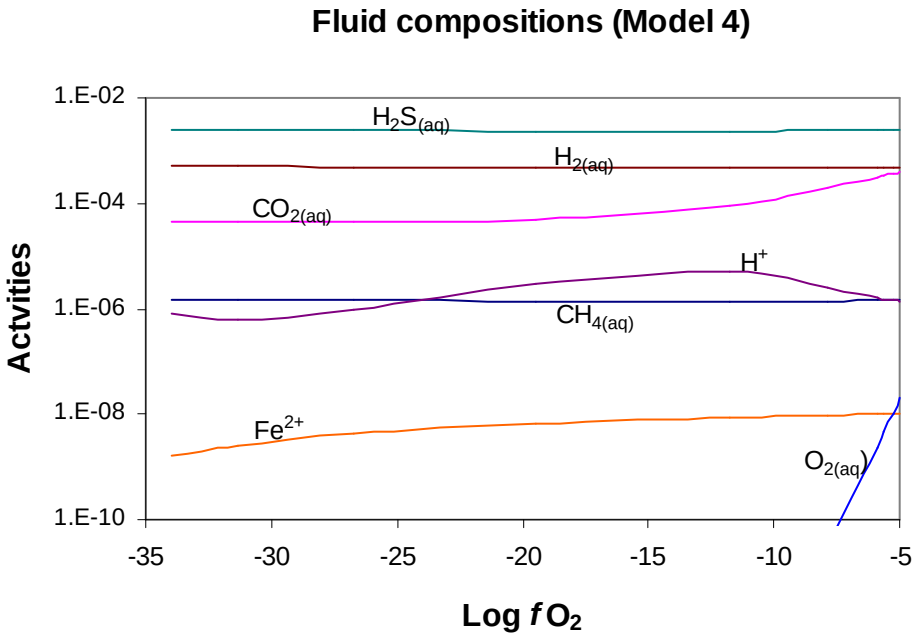

Figure 7: Log-log plot of activities of all relevant species calculated in the H-O-C-S-Fe-system as a result of mixing martian hypothetical hydrothermal fluid and atmosphere. $CO_{2(aq)}$ represents the sum of the $CO_{2(aq)}$ and HCO_3^-. $H_2S_{(aq)}$ represents the sum of $H_2S_{(aq)}$ and $HS^-_{(aq)}$. $a Fe^{3+} \sim 10^{-28}$ and not shown on graph. $aSO_4^{2-} < 10^{-10}$.

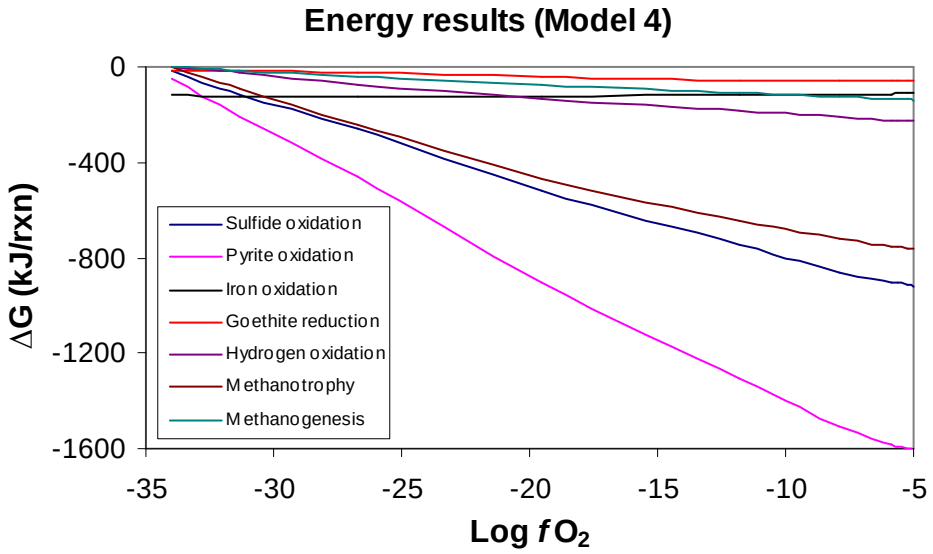

Figure 8: Energy results of chemolithoautotrophic reactions from Table 1 as a function of oxygen fugacity as a result of mixing hypothetical martian hydrothermal fluid and atmosphere. Sulfate and iron reduction (Reactions 3 and 6) have positive Gibbs energy values and are considered not favorable and are not shown on this graph.

Biomass was estimated from the assumptions described in previous sections and are shown in Figure 9 as function of temperature. Only temperatures below 150°C are shown because it is unlikely that organisms would be able to metabolize and grow at temperatures above this based on what we know about the limits for life on Earth [Nealson, 1997; Rothschild and Mancinelli, 2001]. Goethite reduction, methanogenesis, and methanotrophy would have been the reactions able to support the most amount of biomass with ~10^7-10^9 cells/kg hydrothermal fluid.

2.5 Shallow, subsurface hydrothermal system (Model 5)

Another source of chemical disequilibrium for potential microorganisms could have been the interaction of groundwater with hydrothermal fluid. Hydrothermal systems can occur at any depth in the crust where water is in contact with a heat source. The hot, reduced hydrothermal fluid would have risen buoyantly towards the surface and would have been out of equilibrium with cooler, oxidized groundwater. For this model (Model 5), a relatively oxidizing groundwater was mixed with a high temperature (300° C) hydrothermal fluid until a groundwater:hydrothermal fluid ratio of 1000 was reached. The variations in the composition of the fluid during mixing were estimated using a mixing model similar to McCollom and Shock [1997]. The martian hydrothermal fluid starting composition was calculated by the same methods described in Model 4 and the hydrothermal fluid composition is shown in Table 2. The hydrothermal fluid composition was then reacted with increments of the groundwater to simulate the mixing that occurs as hot fluids rise toward the surface and interact with oxidizing groundwater [McCollom and Shock, 1997]. The groundwater composition was obtained from equilibrium between the groundwater calculated in Model 1 and a soil composition derived from Gusev crater measurements [Gellert et al., 2004]. The composition of the groundwater before

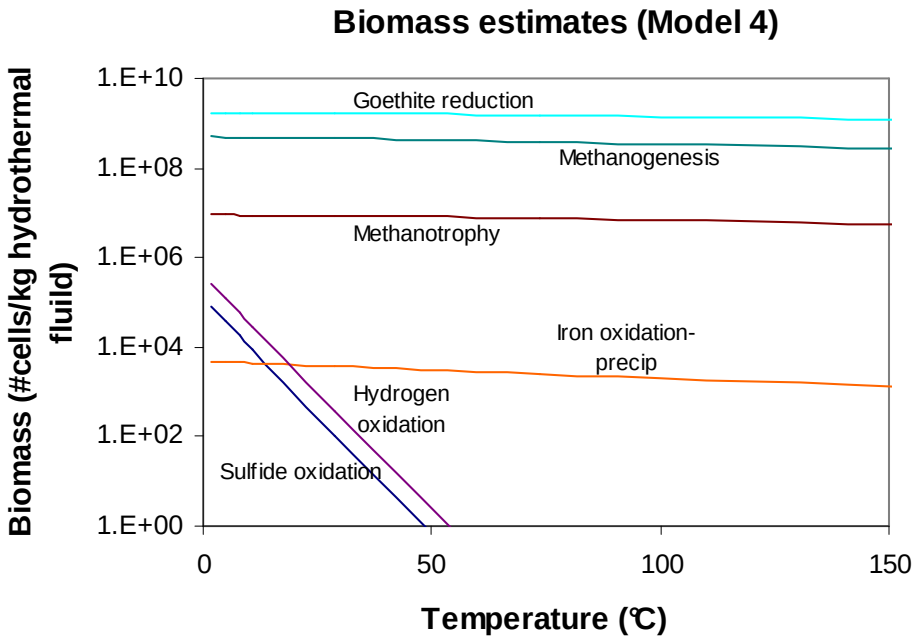

Figure 9: Number of cells/kg hydrothermal fluid as a function of temperature. Temperatures greater than 150°C were not shown as life cannot survive above this temperature. Only reactions that produce more than 1 cell per kg fluid is shown.

mixing is shown in Table 2. The resulting aqueous compositions that result from mixing hydrothermal fluid and groundwater is shown in Figure 10 as a function of groundwater:hydrothermal fluid ratio and equivalently temperature. Minerals were allowed to precipitate and minerals such as pyrite, quartz, gypsum and anhydrite (sulfates), talc, antigorite (clays), and dolomite and magnesite (carbonates) were predicted to precipitate (Table 4).

2.5.1 Energy and biomass results

The results from Figure 10 were used to calculate the amount of energy released from the reactions in Table 1 from Equation 1. The results show that from temperatures of 150°C to 2°C, there would have been a number of reactions that would have been favorable for potential chemolithotrophic organisms. The greatest amount of energy would have been available from the oxidation of pyrite. In this mixing model, pyrite was predicted to precipitate at temperatures less than 150°C. For every mole of pyrite that was oxidized, -1120 to -1257 kJ would have been released for temperatures ranging from 150°C – 2°C, respectively. In this case, the lower temperatures would have created more available energy. As more and more groundwater was added to the system, the oxygen levels increased, whereas the H_2 and CH_4 levels decreased (Figure 10). Even though the anaerobic reactions have lower levels of H_2 and CH_4 at lower temperatures, sulfate reduction, iron reduction and methanogenesis would still have been capable of supplying energy to potential organisms per mole of either S, Fe or C (Figure 11). Looking at the reaction for sulfide oxidation in greater details shows that the reaction is favorable at all temperatures (Figure 12) when expressed in terms of sulfur species reacted. It may be more reasonable to express these energies based on the concentration of the limiting reactant instead [McCollom and Shock, 1997]. In this case, O_2 would have been the limiting reactant.

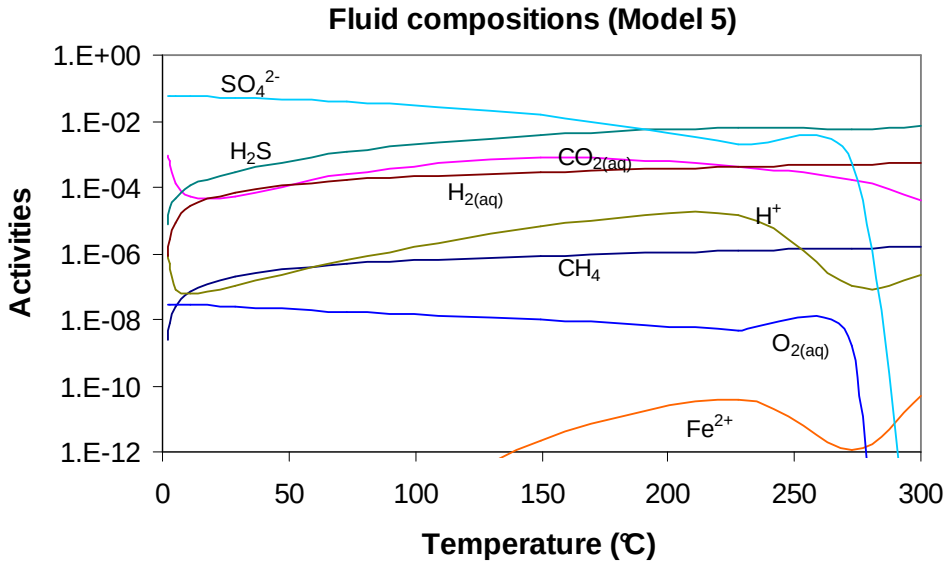

Figure 10: Activities of all relevant species calculated in the H-O-C-S-Fe-system as a result of mixing martian hypothetical hydrothermal fluid and a relatively oxidizing groundwater. $CO_{2(aq)}$ represents the sum of the $CO_{2(aq)}$ and HCO_3^-. $H_2S_{(aq)}$ represents the sum of $H_2S_{(aq)}$ and $HS^-_{(aq)}$. aFe^{3+} ~10^{-28} to ~10^{-21} and not shown on graph.

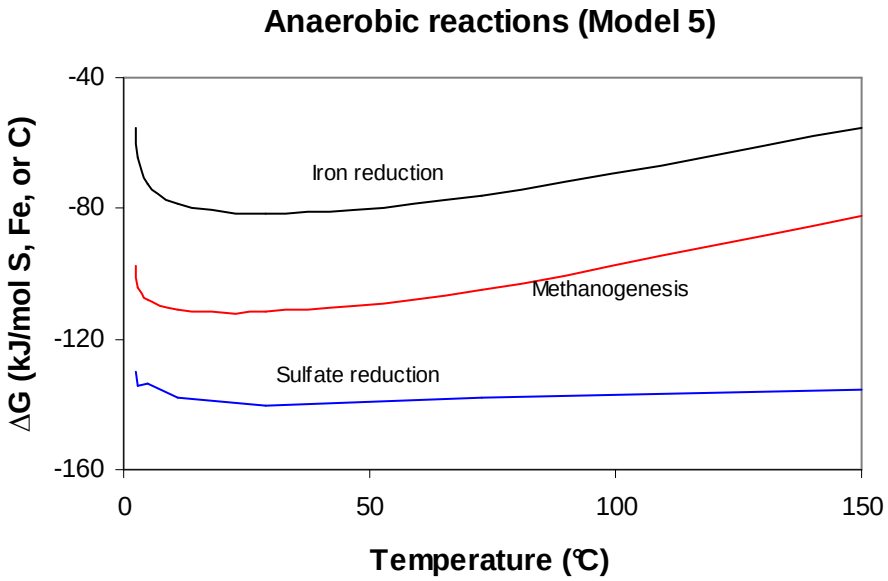

Figure 11: Energy results of anaerobic chemolithoautotrophic reactions from Table 1 as a function of temperature, or equivalently groundwater:hydrothermal fluid ratio, as a result of mixing.

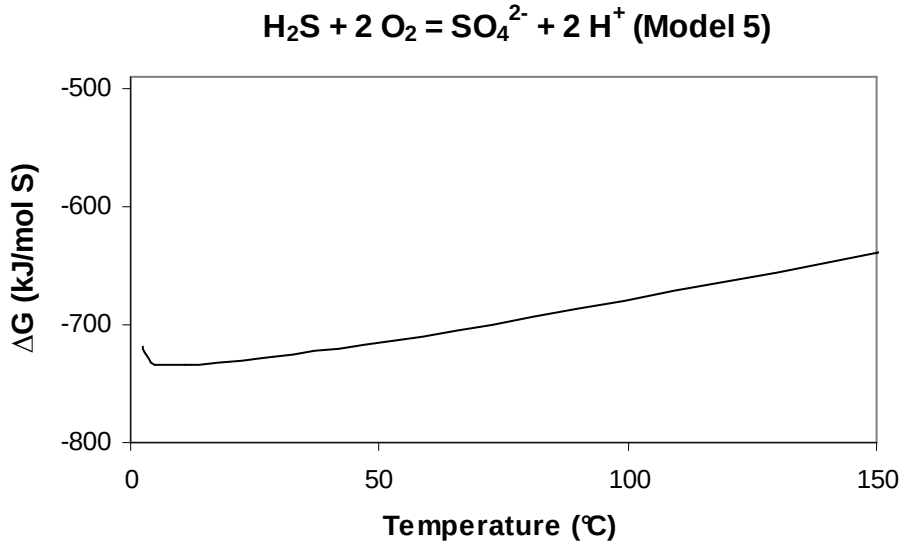

Figure 12: Energy results of sulfide oxidation (Reaction 1, Table 1) as a function of temperature, or equivalently groundwater:hydrothermal fluid ratio, as a result of mixing.

Accounting for stoichiometry, the values in Figure 12 were divided by 2 and multiplied by the concentrations of O_2 of the mixed fluid at each temperature in order to calculate the energy available per kg of mixed fluid. To calculate the energy available from each kg of hydrothermal fluid, the Gibbs energy per kg of mixed fluid was multiplied by the mass of mixed fluid at each temperature. This results in the values shown in Figure 13. Figure 13 shows that the maximum amount of energy available from sulfide oxidation would have been 10.4 J/kg hydrothermal fluid. This can be compared to the work of McCollom and Shock [1997] who evaluated the amount of metabolic energy available from terrestrial hydrothermal systems. They report 760 cal/kg hydrothermal fluid (equivalent to 3180 J/kg hydrothermal fluid), roughly two orders of magnitude higher than the results presented here. This is likely due to their lower O_2(aq) concentration assumed for Mars. Performing the same calculations for methanogenesis resulted in a maximum of 23.3 J/kg of hydrothermal fluid compared to McCollom and Shock [1997] value of 29 J/kg of hydrothermal fluid for the same reaction, which is very similar. Sulfate reduction would have had a maximum of 29.3 J/kg of vent fluid compared to McCollom and Shock [1997] value of 42 J/kg of vent fluid. These calculations represent the total amount of energy available from the metabolic reaction if all of the reactants are consumed.

In terms of biomass estimates and making the same assumptions as described above, all of the reactions except ferrous iron oxidation and ferric iron reduction produce a relatively large number of grams of biomass per kg of vent fluid. Sulfate reduction, for example, could have produced up to 0.084 mg of biomass/kg hydrothermal fluid and methanogenesis would have produced 0.067 mg/kg hydrothermal fluid compared to a reported value of 5 mg/kg fluid for a terrestrial hydrothermal system from McCollom and Shock [1997]. Hydrothermal systems on Earth have fluid fluxes of 5×10^5 kg/hr [Converse, 1984], and if martian hydrothermal systems

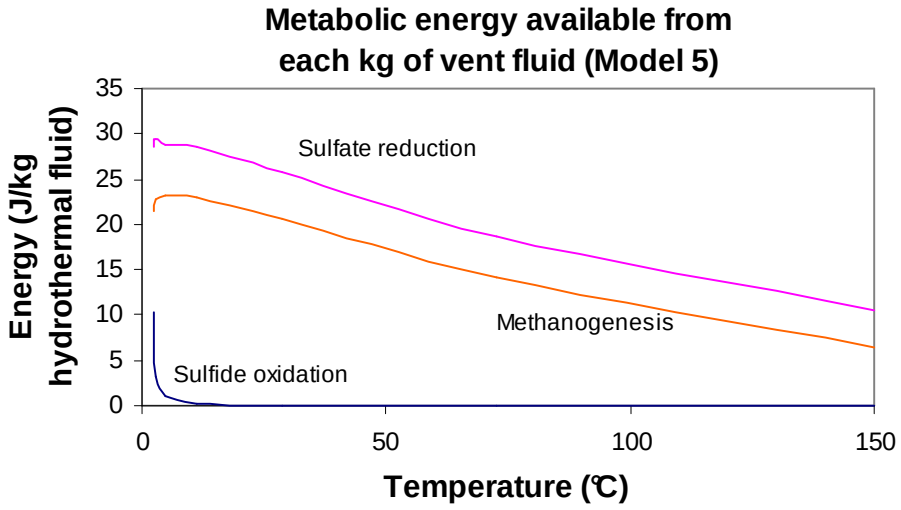

Figure 13: Metabolic energy available from sulfate reduction, sulfide oxidation and methanogenesis for each kg of vent fluid as a result of mixing.

were similar, then the results from Model 5 show that a maximum of 249 grams of biomass could be produced per hour at one martian hydrothermal system. This is essentially identical to the results of Varnes et al. [2003] who predicted that 250 grams of biomass could be produced per hour at an martian individual hydrothermal system with Shergotty as the host rock.

2.6 Deep, subsurface hydrothermal system (Model 6)

Because the composition of martian groundwater is highly unknown, a more reducing groundwater was modeled as an additional end member for the martian groundwater and its potential oxidation states. This type of scenario would have occurred in the martian subsurface where hydrothermal water interacted with groundwater. This model (Model 6) is similar to Model 5 except that the initial groundwater composition is assumed to be more reducing. The composition of the reduced groundwater from Model 3 was also used in this model at a temperature of 60°C (Table 2). Aqueous activities are shown in Figure 14 as a result of mixing the more reducing groundwater with hydrothermal fluid. The predicted precipitated minerals are similar to Model 5 (Table 4).

2.6.1 Energy and biomass results

Mixing a reducing groundwater with a reducing hydrothermal fluid should result in less Gibbs energy for each reaction as there is less redox potential available. The model results show this to be true. Although the Gibbs energies for each reaction per mole of Fe, S, C or H seem to be comparable with model 5, the concentrations of the limiting compounds are much lower (e.g. O_2 is now on the order of $\log fO_2 = -10$ instead of $\log fO_2 = -5$). This results in virtually no energy available per kg of hydrothermal fluid for reactions that require O_2 for oxidation. Sulfate

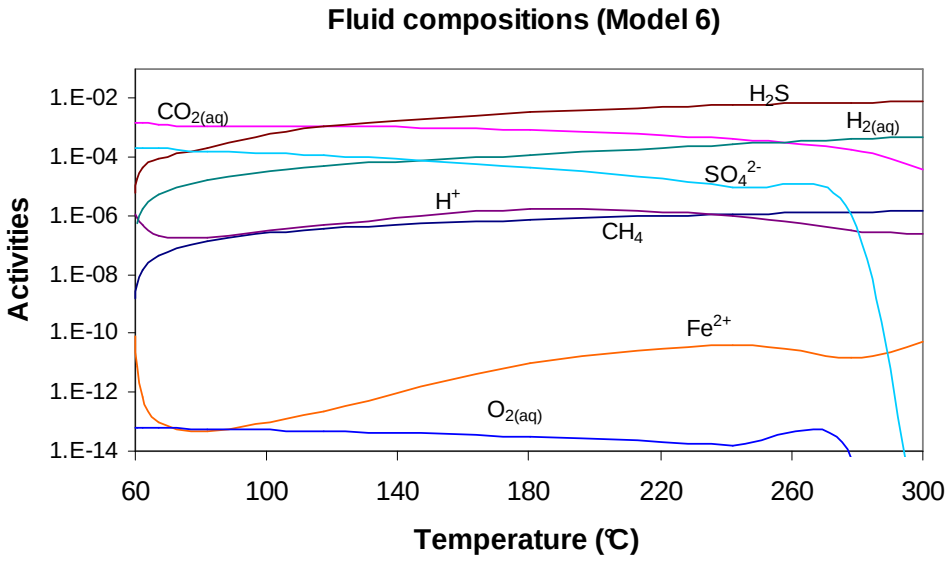

Figure 14: Activities of all relevant species calculated in the H-O-C-S-Fe-system as a result of mixing martian hypothetical hydrothermal fluid and a relatively reducing groundwater. $CO_{2(aq)}$ represents the sum of the $CO_{2(aq)}$ and HCO_3^-. $H_2S_{(aq)}$ represents the sum of $H_2S_{(aq)}$ and $HS^-_{(aq)}$. aFe^{3+} ~10^{-28} to ~10^{-23} and not shown on graph.

reduction can, however, supply a maximum of 12 J/kg hydrothermal fluid for martian systems compared to 42 J/kg hydrothermal systems for terrestrial settings [McCollom and Shock 1997], which are similar results. Sulfate reduction and methanogenesis are the only reactions that would have produced a substantial amount of biomass with 0.037 mg biomass/kg hydrothermal fluid and 0.034 mg biomass/kg hydrothermal fluid, which is slightly less than what was calculated for Model 5.

2.7 Summary of all reaction path models

A summary of the Gibbs energies for each reaction and each model is shown in Figure 15. Note that the majority of the Gibbs energies for each model are comparable when expressed in terms of kJ per mole Fe, S or C species. All biomass estimates from this study are shown in Table 9 for the aqueous components and Table 6 for the solid components. The overall results of each reaction path model show that all the aqueous settings evaluated in this study had the potential to be habitable based on the amounts of energy that would have been available from chemical reactions, but not all reactions would have been biologically useful. Each environment has a set of reactions that would have been more favorable than others. In the case of aqueous weathering at or near the surface (Models 1 and 2), aerobic reactions would have been the likely reactions to have gone forward. After taking into account the availability of limiting reactants and biomass assumptions, the sum of biomass from all chemolithotrophic reactions for Model 1 shows that ~10^5 cells/kg fluid could have been sustained. This value represents a maximum amount of biomass as reactants from all ten reactions would have been in competition and consumed. Model 2 biomass estimates are slightly higher than Model 1, but are essentially the same with ~10^5 cells/kg fluid. Model 3 had the potential to produce a maximum of ~10^4 cells/kg

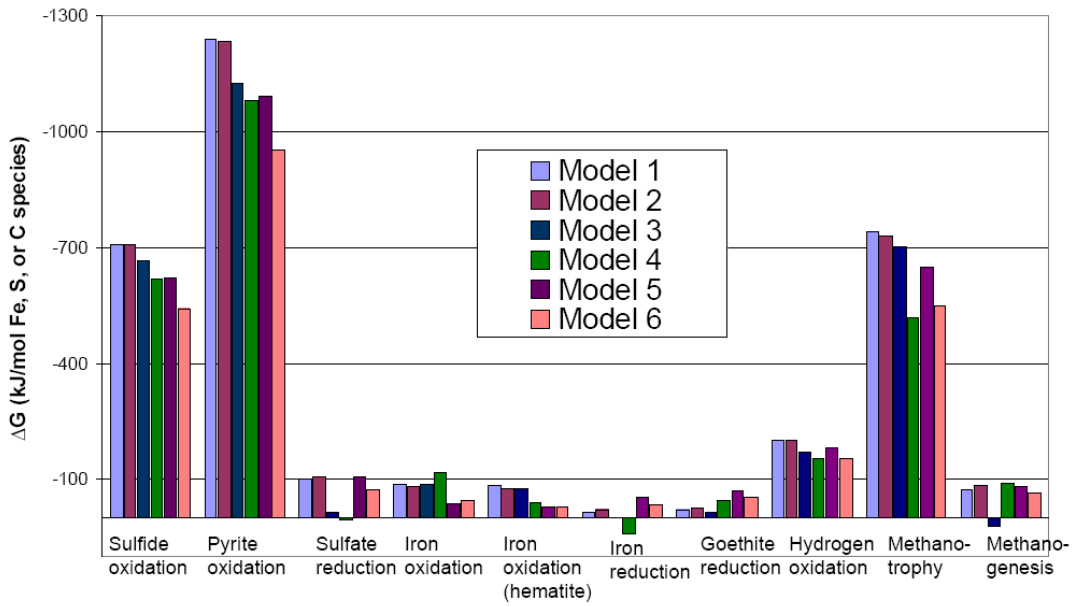

Figure 15: All reactions from Table 1 are shown with the Gibbs energy for each Model. Gibbs energy is expressed in kJ/mol Fe, S, or C species. Models 1 and 2 show values calculated from Equation 1 at T = 2°C averaged over all water:rock ratios. Model 3 was calculated at T = 60°C averaged over all water:rock ratios. Gibbs energies were calculated at T = 2-150°C for Models 4 and 5 and this graph shows the average of those values. Model 6 shows the average energies calculated at T = 60-150°C.

Table 9: Biomass estimates for each Model. Values are expressed in terms of number of cells/kg fluid.

Rxn	Equation	**Model 1** (Shallow aquifer-present)	**Model 2** (Shallow aquifer-past)	**Model 3** (Deep aquifer)	**Model 4** (Yellow-stone)	**Model 5** (HVF mixed w/ ox. GW)	**Model 6** (HVF mixed w/ red. GW)
1	$H_2S + 2\ O_{2(aq)} = SO_4^{2-} + 2\ H^+$	7.75E+02	1.28E+03		2.00E+04	1.73E+07	3.17E+01
2	$Pyrite + H_2O + 3.5\ O_{2(aq)} = Fe^{2+} + 2\ SO_4^{2-} + 2\ H^+$	5.81E+04	5.78E+04		2.00E+04	1.73E+07	3.17E+01
3	$SO_4^{2-} + 2\ H^+ + 4\ H_{2(aq)} = H_2S_{(aq)} + 4\ H_2O$	1.03E+04	1.02E+04	1.65E+03		6.94E+08	3.13E+08
4	$Fe^{2+}\ 0.25\ O_{2(aq)} + H^+ = Fe^{3+} + 0.5\ H_2O$	5.97E+04	5.27E+04				2.39E+01
5	$Fe^{2+} + H_2O + 0.25\ O_{2(aq)} = 0.5\ Hematite + 2\ H^+$	5.73E+04	5.06E+04		3.62E+03	5.05E+00	1.53E+01
6	$Fe^{3+} + 0.5\ H_{2(aq)} = Fe^{2+} + H^+$						
7	$Goethite + 2\ H^+ + 0.5\ H_{2(aq)} = 2\ H_2O + Fe^{2+}$	1.28E+04	2.04E+04	1.14E+04	1.57E+09	3.37E+09	1.63E+09
8	$H_{2(aq)} + 0.5\ O_{2(aq)} = H_2O$	3.05E+04	7.82E+04	1.01E+00	7.03E+04	7.31E+07	1.28E+02
9	$CH_{4(aq)} + 2\ O_{2(aq)} = 2\ H_2O + CO_{2(aq)}$	1.48E+02	1.40E+02		8.07E+06	1.19E+07	3.23E+01
10	$CO_{2(aq)} + 4\ H_{2(aq)} = 2\ H_2O + CH_{4(aq)}$	7.20E+03	7.98E+03		4.35E+08	5.37E+08	2.71E+08
	TOTAL	2.37E+05	2.80E+05	1.30E+04	2.00E+09	4.72E+09	2.21E+09

Values less than 1 cell/kg fluid were not reported. HVF = hydrothermal vent fluid; ox. = oxidized; red. = reduced; GW = groundwater. Also, it was assumed that 1 cell weighs 1 x 10^{-13} grams [Phelps et al., 1994].

fluid. Model 4 had the potential to produce a maximum of ~2 x 10^9 cells/kg hydrothermal fluid. Models 5 had the potential to produce a maximum of ~5 x 10^9 cells/kg hydrothermal fluid and seems to have been the most favorable type of scenario for potential chemolithoautotrophs with eight out of the ten reactions able to produce a relatively large number of cells (10^7-10^9 cells/kg hydrothermal fluid). Sulfate reduction, goethite reduction, and methanogenesis are the only reactions for Model 6 that would have produced a significant number of cells (~2.2 x 10^9 cells/kg hydrothermal fluid).

Putative basalt aquifers, hot springs and subsurface hydrothermal systems on Mars all prove to have been environments that could have been inhabited by potential chemolithoautotrophic organisms. We compare the maximum overall biomass estimates of all the environments modeled in this study in order to determine which environment may have been more or less habitable. When we examine the biomass estimates in terms of the amount of fluid that would have been available (either hydrothermal vent fluid or groundwater), we conclude that subsurface hydrothermal systems would have been the most habitable type of environment followed by a hot spring and then a basalt aquifer (see Table 9). This, however, may not be a fair assessment as potential organisms would have likely been sustained by living on or within the basalt in the aquifer; thus, we need to include the biomass estimates from the solid-mineral components for the basaltic aquifer environments. Unfortunately, this is not a straightforward relationship as the energy calculated per kg of fluid cannot be directly compared to the energy calculated per kg of rock altered. For this reason, we make assumptions about global hydrothermal fluid fluxes and crustal production rates in order to draw comparisons between all six environments in terms of the amount of biomass that could have been sustained per hour for each system. Martian hydrothermal fluid flux was calculated by assuming that the martian

volcanism rate is 100 times smaller than the terrestrial volcanism rate [Jakosky and Shock, 1998], thus a global, terrestrial hydrothermal fluid flux of 3×10^{13} kg/yr assumes a martian hydrothermal fluid flux of 3×10^{11} kg/yr. Based on this fluid flux, we calculated that Model 4 could have produced 6×10^{7}g biomass/yr; Model 5 could have produced 1.4×10^{8}g biomass/yr; and Model 6 could have produced 6.6×10^{7}g biomass/yr globally. We used a global crustal production rate of basalt on Mars of 7.4×10^{11}kg/yr. This equates to 4.4×10^{11}g biomass/yr for Model 1; 4.8×10^{11}g biomass/yr for Model 2; and 3.5×10^{11}g biomass/yr for Model 3. Globally, this shows that basalt aquifers would have had the most biological potential, followed by hydrothermal systems, and hot spring would have had the least biological potential. This assumes that all of the reactant produced (hydrothermal fluid or basalt) would have been used up entirely.

CHAPTER 3

DISCUSSION

3.1 Terrestrial Analogs

In order to be able to predict which types of life might have existed on Mars, we discuss terrestrial analogs of similar environments modeled in this study. Each of the environments that we modeled can be applied to a terrestrial site that is known to support chemoautotrophic activity on Earth.

Chemical disequilibrium arises in terrestrial hydrothermal systems from the mixing of the reduced materials in the hydrothermal fluid with cooler groundwater that supplies inorganic energy sources for chemolithoautotrophs. On Earth, hydrothermal systems are abundant with life and host a diverse range of microorganisms with diverse metabolisms. For example, large numbers of sulfur-oxidizing chemolithotrophs such as *Thiobacillus*, *Thiomicrospira*, *Thiothrix*, and *Beggiatoa* are found in and around terrestrial hydrothermal vents [Madigan et al., 2003]. Some vents are also known to contain hydrogen-oxidizing bacteria and iron-oxidizing bacteria. This study showed that a hypothetical martian hydrothermal fluid (Model 5) may have had similar fluid chemistry to terrestrial hydrothermal fluid, therefore we suggest that potential martian organisms also would have taken advantage of similar metabolic pathways. We suggest that if life ever evolved on Mars in subsurface hydrothermal systems, then organisms such as the ones mentioned above would be the types of organisms for which we would want to search. It is unknown if hydrothermal environments were ever active in the subsurface of Mars in the past or present, but the search for this type of life may prove to be difficult simply because it would have to be detected many meters below the surface.

Yellowstone National Park can also serve as a terrestrial analog for Model 4 from this study. Yellowstone is an environment that contains hydrothermal water that is heated from a volcanic source and discharges at the surface either as geysers, hot springs or fumaroles. Most microbial biomass in these systems is dominated by H_2-metabolizing organisms with sulfur oxidizers playing a more minor role further away from the heat source [e.g., Spear et al., 2005]. Specific types of chemolithotrophs that have been identified in hot springs at Yellowstone include *Aquificales, Thermotogales, Thermus, Deinococcus* and *Thermodesulfobacteria.* On Mars, there are sites like Gusev Crater that have mineralogy indicative of possible discharge of hydrothermal fluids onto the surface. Any location on Mars with evidence of hydrothermal fluid reaching the surface would be important astrobiologically based on the thermodynamic calculations from this study and from this terrestrial analog.

The last type of terrestrial analog relevant to this research is a basalt aquifer. Basalt aquifers on Earth harbor a diverse array of bacteria that include anaerobes such as sulfate reducers and methanogens hundreds of meters below the surface as well as aerobic bacteria [Madigan et al., 2003]. These types of organisms have been identified in basalts from the Columbia River Basin, for example [Stevens and McKinley, 1995]. H_2-metabolizing organisms seem to play a role at this type of setting as well. Basalt aquifers most likely existed in the past and may even exist in the subsurface today. Again, searching for subsurface life (extant or extinct) on Mars is not ideal for current or future astrobiological missions. In the future, however, missions that are able to drill many meters below the surface may want to start their search for life with H_2-metabolizing chemolithotrophs.

3.2 Mars Exploration Rover application

The results from this study can also be applied to the Mars Exploration Rover (MER) landing sites. Gusev Crater is described as a 160-km crater with past aqueous activity. There is evidence of high concentrations of silica which implies that hydrothermal fluid may have discharged onto the surface. The silica deposits are also in close association with ferric sulfates that are probably of hydrothermal origin [Squyres et al., 2008]. The chemical environment at Gusev Crater may have been formed from fumarolic and hydrothermal deposit [Yen et al., 2008] similar to an environment like Yellowstone. Our results imply that if Gusev Crater was indeed an environment where hydrothermal fluid discharged onto the surface, as in our Model 4, then chemolithoautotrophic reactions such as ferric iron reduction and methanogenesis could have been the most favorable reactions. At an environment like Gusev Crater, a maximum of ~0.2 mg biomass/kg hydrothermal fluid could have potentially been produced, given the assumptions in Model 4.

Meridiani Planum has a complicated diagenetic history but has been inferred by the Mars Exploration Rover (MER) team to be a place where there was once acidic groundwater and arid, oxidizing conditions [Squyres et al., 2004; *Squyres* and Knoll, 2005]. The *Opportunity* Rover detected sand-sized grains composed of Mg-, Ca-, and Fe-sulfates, which most likely formed from an aqueous solution of sulfuric acid which reacted with a basaltic source material with subsequent evaporation [Squyres et al., 2004; Squyres et al., 2006; Squyres and Knoll, 2005]. They suggest, however, that the sulfate-rich sandstones observed at Meridiani were blown in from a prior environment that is unknown to date. After deposition of the sandstones, the outcrops at Meridiani interacted with substantial amounts of acidic groundwater in order to produce the hematite-bearing concretions [Squyres et al., 2006]. A high concentration of sulfur and unique textures in rock outcrops were detected and indicate the extended presence of surface

or near-surface water over a large region of Mars [Squyres et al., 2004; Hynek, 2004]. Results from Eagle crater at Meridiani Planum also show that the rocks have been exposed to surface water at shallow depths, and primary igneous minerals are not readily identified at Eagle crater [Squyres et al., 2004], suggesting a substantial degree of low-temperature chemical alteration. Our results imply that if Meridiani Planum was a location where shallow water interacted with low-temperature basalt, as in our Model 2, then ~650mg biomass/kg basalt could have been produced if all of the basalt underwent alteration. Iron oxidation, iron reduction, sulfide oxidation, and hydrogen oxidation would have been the reactions that supported the most amount of biomass.

Overall, both MER sites had the potential to be habitable based on energy availability. A general assessment shows that the Opportunity site would have had more biological potential than the Spirit site as a martian system with altered solid minerals proves to be more biologically useful than a putative martian hot spring.

3.3 Mars Science Laboratory potential landing sites

Much of the surface and subsurface of Mars is yet to be explored by rovers or landers. Future missions to Mars are likely to be driven by the search for life past or present, thus locations that had/have the greatest biological potential should be at the top of the list. Cases are made repeatedly for potential landing sites, and this study can be used to further constrain which locations may have been more likely to have been habitable.

The Mars Science Laboratory is the next mission, scheduled to launch in the fall of 2011. Its primary mission is to assess the habitability of Mars by determining if a specific area ever had the potential to develop life and preserve evidence of that life. The mission team has been

progressively narrowing down possible landing sites [Grant et al., 2010], and as of this writing, four possible landing sites remain as candidates. These four potential landing sites are discussed below as we describe each potential landing site's geological setting and explain why it is argued to have been a potential habitable environment. All of this information was drawn from the Mars Science Laboratory Landing Sites websites (http://marsoweb.nas.nasa.gov/landingsites/index.html and http://webgis.wr.usgs.gov/msl/). Furthermore, we apply our specific model results to each potential landing site in order to assess which site may have been more or less habitable than another.

3.3.1 Brief Overview of each potential site

Eberswalde Crater is a large crater (~65 km) that contains evidence of ancient deltaic deposits. This delta most likely formed by rivers flowing into a large standing body of water [Lewis and Aharonson, 2006; Pondrelli et al., 2008]. This process requires a lot of water for sediment deposition and is therefore considered to be a potentially habitable environment. Clay minerals and extensive phyllosilicates have also been detected from orbiters in the sediments. Mg/Fe- smectite has been detected which is indicative of reducing conditions.

Gale Crater contains a 5-km-high mound of layered materials in the center of a 150 km crater. The layers contain a wide range of mineralogy that includes sulfates and phyllosilicates [Milliken et al., 2010]. Fe-rich smectite clay lies in the lower strata (reducing) with sulfates in the overlying strata (oxidizing). Some of the strata in the 5 km-high mound were thought to have been deposited in a subaqueous setting, which means that for some periods during its history, Gale Crater hosted a lake. The higher sections of the layered materials are likely to have been deposited in a subaerial setting.

Holden Crater is another crater that shows that a large amount of water was once present on Mars in the form of a lake bed [Grant et al., 2008]. This crater also contains a channel, Uzboi Vallis, that runs into it and has deposits at its mouth. It is likely that water carved deep gullies in the crater and transported sediment onto the floor of a lakebed which was deposited ~3 billion years ago. Today, it is evident that the cratered floor is mantled by layered and fan deposits [Pondrelli et al., 2005]. Phyllosilicates and Fe/Mg smectites have been detected from orbiters.

Mawrth Vallis itself is an ancient outflow channel carved by catastrophic floods. Layered cliffs are rich in clay minerals such as phyllosilicates. There is evidence for intense alteration in the form of hydrated silica and kaolinite [Wray et al., 2008; Michalski and Noe Dobrea, 2007]. In order for kaolinite to form, a lot of water and good circulation are needed to transport metal ions away. Typically kaolinite forms under mild temperatures with water at or near the surface that interacts with basalt. Ferrous iron overlies nontronite (ferric) which is consistent with hydrothermal activity. Also, montmorillinite and Fe/Mg smectite have been detected in the layers. This location contains a high abundance of hydrated minerals and also includes some redox potential from various oxidation states of Fe.

3.3.2 Application of our results

We can assess all four landing sites in terms of energy availability for chemolithotrophic types of life. Based on our earlier results, sites with more chemical disequilibrium and have evidence of redox chemistry had more potential to be habitable.

Eberswalde Crater and Holden Crater both have evidence for fluvial processes, but are considered here to be the lowest priority for the search of a habitable environment. Although there is evidence of standing bodies of water and fluvial processes, there is no evidence for any

redox chemistry or chemical disequilibrium having occurred that would have been able to support chemolithotrophs. Lakes and rivers on Earth host a diversity of life forms, most of which are constrained to photosynthetic organisms. Deep in the bottom of the lake where no oxygen is present (anoxic), anaerobic bacteria such as methanogens are found. They, however, are likely using electron donors from reducing organic compounds which was not likely the case for Mars. The identification of clays shows that water was present, but the precipitation of kaolinite or montmorillinite, for example, have no redox chemistry, therefore are not biologically useful from a thermodynamic point of view.

Gale Crater and Mawrth Vallis are considered here to be higher priority for the search of habitable environments because they each have evidence for one type of redox chemistry. Gale Crater shows evidence for both oxidizing and reducing conditions in the form of reduced smectite and oxidized sulfates. Reduced and oxidized iron (nontronite) has been detected in Mawrth Vallis. Nontronite can form from the weathering of basalt at low temperatures or precipitate from hydrothermal fluids. If there was hydrothermal fluid circulating in Mawrth Vallis, then potential chemolithotrophs would have had numerous energy sources.

A summary is shown in Table 10. Currently, we suggest that sites with lacustrine settings or fluvial channels would not harbor enough geochemical energy to support chemosynthesis. Sites with evidence of hydrothermal alteration and interesting redox chemistry will prove to have more biological potential based on thermodynamic energy requirements.

3.4 Caveats about geochemical modeling

Ancient groundwater and hydrothermal fluid compositions are highly uncertain on Mars, so geochemical models are a useful tool when trying to determine what those values may have

Table 10: Summary table for each MSL potential landing site and this study's priority ranking.

NAME	TARGET	RATIONALE	PRIORITY
Holden Crater	Fluvial layers, phyllosilicates	No evidence for any redox chemistry or chemical disequilibrium having occurred that would have been able to support chemolithotrophs	Low
Eberswalde Crater	Delta, phyllosilicates	Clays show that water was present, but no redox chemistry is involved, therefore not biologically useful from a thermodynamic point of view	Low
Mawrth Vallis	Layered phyllosilicates, oxidized and reduced Fe, hydrothermal?	Reduced and oxidized iron (nontronite) has been detected. Nontronite can form from the weathering of basalt at low temperatures or precipitate from hydrothermal fluids	High
Gale Crater	Layered sulfates, phyllosilicates, Fe-smectite	Evidence for both oxidizing and reducing conditions in the form of reduced smectite and oxidized sulfates	High

been. It is difficult to put a value on the uncertainty that goes into calculating the fluid compositions, but it should be noted that the fluid compositions are hypothetical and are based on many assumptions such as host rock composition, temperature, atmospheric inputs, and water:rock ratio. Any variation in any of these inputs will affect the resulting fluid composition, and thus will affect the Gibbs energies. The more chemical information that is known from the martian environment, the more accurate the models become. With that said, geochemical models can predict mineral stability and the mineralogy data from the model can be used as a ground truth to determine the accuracy of the model. These models also can be easily adapted as new information is obtained and make the models more accurate. The compositions of basalt and the present-day atmosphere are constrained well on Mars, and with more mineralogical data at the surface, it is possible to know how well the models are representing the actual past physical environment.

At first glance, the Gibbs energies for the majority of the reactions appear to be favorable when expressed in terms of kJ per mole of S, Fe, C or H species. Once the concentration of the limiting factor is taken into account, the Gibbs energies decline drastically. This is because the concentrations for the limiting reactants are extremely low in most cases. This severely lowers the biological potential of the system, but is probably a more realistic way to evaluate each metabolic energy source. Also, the calculations for biomass production are based on the assumption that each reaction is able to consume all of the reactant, which is probably not the case if more than one reaction is occurring at the same time and place. The reactions may have been competing for available reactants, thus our calculations represent maximum energy and biomass yields.

CHAPTER FOUR

CONCLUSIONS

Thermodynamic reaction path calculations reveal that several different potential types of environments on Mars had sufficient metabolic energy sources for putative chemolithoautotrophs. Globally, when a hydrothermal fluid flux and crustal production rate for Mars is considered, a shallow basalt aquifer proves to be the environment with the most biological potential. This is followed by subsurface hydrothermal which suggests that martian biomass estimates may have been less than, but comparable to, terrestrial values. Therefore, the subsurface of Mars is considered to have/had a large biological potential. Environments where hydrothermal fluid reached the surface of Mars, such as hot springs, may have also had a substantial amount of energy sources for chemolithotrophs, but is considered here to have had the least biological potential of all the environments analyzed in this study.

On Earth all three of these types of environments harbor a diversity of microorganisms, and based on the geochemistry and thermodynamics for martian systems, it is reasonable to suspect that the amount of potential martian chemolithoautotrophic organisms would have been comparable to those found in terrestrial environments. It is important to note that when searching for life elsewhere in the solar system, the detection of water cannot simply be the only factor for assessing habitability. Available metabolic energy sources, as well water, can offer an additional constraint on potential habitability and aid the search for life elsewhere in the solar system.

BIBLIOGRAPHY

Bach, W., and K. J. Edwards (2003), Iron and sulfide oxidation within the basaltic ocean crust: implications for chemolithoautotrophic microbial biomass production, *Geochimica et Cosmochimica Acta, 67*(20), 3871-3887.

Baker, V.R, M.H. Carr, V.C. Gulick, C.R. Williams, and M.S. Marley (1992), Channels and valley networks, *Mars* (A93-27852 09-91), 493-522.

Bethke, C. M. (1996), *Geochemical Reaction Modeling, Concepts and Applications*, Oxford University Press, Inc., New York.

Bibring, J., et al (2005), Mars Surface Diversity as Revealed by the OMEGA/Mars Express Observations, *Science, 307*(5715), 1576-1581, doi: 10.1126/science.1108806.

Bibring, J., et al (2006), Global Mineralogical and Aqueous Mars History Derived from OMEGA/Mars Express Data, *Science, 312*(5772), 400-404, doi: 10.1126/science.1122659.

Boston, P. J., M. V. Ivanov, and C. P. McKay (1992), On the possibility of chemosynthetic ecosystems in subsurface habitats on Mars, *Icarus, 95*(2), 300-308, doi: DOI: 10.1016/0019-1035(92)90045-9.

Cabrol, N. A., E. A. Grin, R. Landheim, R. O. Kuzmin, and R. Greeley (1998), Duration of the Ma'adim Vallis/Gusev Crater Hydrogeologic System, Mars, *Icarus, 133*(1), 98-108, doi: DOI: 10.1006/icar.1998.5914.

Cabrol, N. A., and E. A. Grin (1999), Distribution, Classification, and Ages of Martian Impact Crater Lakes, *Icarus, 142*(1), 160-172, doi: DOI: 10.1006/icar.1999.6191.

Carr, M. H., and M. C. Malin (2000), Meter-Scale Characteristics of Martian Channels and Valleys, *Icarus, 146*(2), 366.

Carr, M. H., and G. D. Clow (1981), Martian Channels and Valleys - their Characteristics, Distribution, and Age, *Icarus, 48*(1), 91-117.

Chapelle, F. H., K. O'Neill, P. M. Bradley, B. A. Methe, S. A. Ciufo, L. L. Knobel, and D. R. Lovley (2002), A hydrogen-based subsurface microbial community dominated by methanogens, *Nature, 415*(6869), 312-315, doi: 10.1038/415312a.

Christensen, P., J. Bandfield, R. Clark, K. Edgett, V. Hamilton, T. Hoefen, H. Kieffer, R. Kuzmin, M. Lane, and M. Malin (2000), Detection of crystalline hematite mineralization on Mars by the Thermal Emission Spectrometer- Evidence for near-surface water, *J. Geophys. Res., 105*(E4), 9623-9642.

Converse, D. R., H. D. Holland, and J. M. Edmond (1984), Flow rates in the axial hot springs of the East Pacific Rise (21°N): Implications for the heat budget and the formation of massive sulfide deposits, *Earth Planet.Sci.Lett., 69*(1), 159-175, doi: DOI: 10.1016/0012-821X(84)90080-3.

Craddock, R. A., and A. D. Howard (2002), The case for rainfall on a warm, wet early Mars, *J.Geophys.Res., 107*(E11), 5111.

Delaney, J., S. Sutton, and M. Dyar (1998), Variable oxidation states of iron in martian meteorites, *Lunar Planet. Sci, Abstract 1241*.

Edwards, K. J., W. Bach, and T. M. McCollom (2005), Geomicrobiology in oceanography: Microbe–mineral interactions at and below the seafloor, *Trends in Microbiology, 13*(9), 449-456.

Ehlmann, B. L., et al (2008), Orbital Identification of Carbonate-Bearing Rocks on Mars, *Science, 322*(5909), 1828-1832, doi: 10.1126/science.1164759.

Ehlmann, B. L., et al (2009), Identification of hydrated silicate minerals on Mars using MRO-CRISM: Geologic context near Nili Fossae and implications for aqueous alteration, *J.Geophys.Res., 114*, E00D08.

Formisano, V., S. Atreya, T. Encrenaz, N. Ignatiev, and M. Giuranna (2004), Detection of Methane in the Atmosphere of Mars, *Science, 306*(5702), 1758-1761, doi: 10.1126/science.1101732.

Fisk, M. R., and S. J. Giovannoni (1999), Sources of nutrients and energy for a deep biosphere on Mars, *J. Geophys. Res., 104*(E5), 11805-11816.

Gellert, R., et al (2004), Chemistry of Rocks and Soils in Gusev Crater from the Alpha Particle X-ray Spectrometer, *Science, 305*(5685), 829-832, doi: 10.1126/science.1099913.

Gooding, J. L. (1992), Soil mineralogy and chemistry on Mars: Possible clues from salts and clays in SNC meteorites, *Icarus, 99*(1), 28-41.

Grant, J. A., M. P. Golombek, J. P. Grotzinger, S. A. Wilson, M. M. Watkins, A. R. Vasavada, J. L. Griffes, and T. J. Parker (2010), The science process for selecting the landing site for the 2011 Mars Science Laboratory, *Planet.Space Sci., In Press, Corrected Proof*, doi: DOI: 10.1016/j.pss.2010.06.016.

Grant, J. A., R. P. Irwin, J. P. Grotzinger, R. E. Milliken, L. L. Tornabene, A. S. McEwen, C. M. Weitz, S. W. Squyres, T. D. Glotch, and B. J. Thomson (2008), HiRISE imaging of impact megabreccia and sub-meter aqueous strata in Holden Crater, Mars, *Geology, 36*(3), 195-198, doi: 10.1130/G24340A.1.

Heijnen, J., and J. van Dijken (1992), In search of a thermodynamic description of biomass yields for the chemotrophic growth of microorganisms, *Biotechnol.Bioeng., 39*(8), 833-858.

Hernandez, M. E., and D. K. Newman (2001), Extracellular electron transfer, *Cellular and Molecular Life Sciences, 58*(11), 1562.

Hynek, B. M. (2004), Implications for hydrologic processes on Mars from extensive bedrock outcrops throughout Terra Meridiani, *Nature, 431*(7005), 156-159.

Jakosky, B. M., and E. L. Shock (1998), The biological potential of Mars, the early Earth, and Europa, *J.Geophys.Res., 103*(E8), 19359-19364.

Jepsen, S. M., J. C. Priscu, R. E. Grimm, and M. A. Bulluck (2007), The potential for lithoautotrophic life on Mars: Application to shallow interfacial water environments, Astrobiology, 7(2), 342-354. DOI: 10.1089/ast.2007.0124.

Kasting, J. F. (1991), CO2 condensation and the climate of early Mars, *Icarus, 94*, 1-13.

Krasnopolsky, V. A., and P. D. Feldman (2001), Detection of Molecular Hydrogen in the Atmosphere of Mars, *Science, 294*(5548), 1914-1917, doi: 10.1126/science.1065569.

Lewis, K. W., and O. Aharonson (2006), Stratigraphic analysis of the distributary fan in Eberswalde crater using stereo imagery, *J.Geophys.Res., 111*(E6), E06001.

Link, L. S., B. M. Jakosky, and G. D. Thyne (2005), Biological potential of low-temperature aqueous environments on Mars, *International Journal of Astrobiology, 4*(02), 155-164.

Lowell, P. (1896), *Mars*, Longmans, Green and Co., London.

Madigan, M. T., J. Martinko, and J. Parker (Eds.) (2003), *Brock Biology of Microorganisms.*, 10th ed., Pearson Education, Inc: Prentice Hall, Upper Saddle River, NJ.

Malin, M. C., and K. S. Edgett (2000), Evidence for recent groundwater seepage and surface runoff on Mars, *Science, 288*(5475), 2330-2335.

Malin, M. C., and K. S. Edgett (2003), Evidence for Persistent Flow and Aqueous Sedimentation on Early Mars, *Science, 302*(5652), 1931-1934, doi: 10.1126/science.1090544.

Malin, M. C., K. S. Edgett, L. V. Posiolova, S. M. McColley, and E. Z. N. Dobrea (2006), Present-Day Impact Cratering Rate and Contemporary Gully Activity on Mars, *Science, 314*(5805), 1573-1577, doi: 10.1126/science.1135156.

Mathez, E.A. (1979), Sulfide relations in Hole 418A flows and sulfur contents of glasses, In *Initial Reports of the Deep Sea Drilling Project, 51-53*, 1069-1085.

McCollom, T. M., and E. L. Shock (1997), Geochemical constraints on chemolithoautotrophic metabolism by microorganisms in seafloor hydrothermal systems, *Geochimica et Cosmochimica Acta, 61*(20), 4375-4391.

McCollom, T. M. (1999), Methanogenesis as a potential source of chemical energy for primary biomass production by autotrophic organisms in hydrothermal systems on Europa, *J. Geophys. Res., 104*(NO. E12), 30,729.

McCollom, T. M. (2000), Geochemical constraints on primary productivity in submarine hydrothermal vent plumes, *Deep Sea Research Part I: Oceanographic Research Papers, 47*(1), 85-101.

Mcsween, H. Y. (1994), What we have Learned about Mars from Snc Meteorites, *Meteoritics, 29*(6), 757-779.

Michalski, J. R., and E. Z. Noe Dobrea (2007), Evidence for a sedimentary origin of clay minerals in the Mawrth Vallis region, Mars, *Geology, 35*(10), 951-954, doi: 10.1130/G23854A.1.

Milliken, R. E., J. P. Grotzinger, and B. J. Thomson (2010), Paleoclimate of Mars as captured by the stratigraphic record in Gale Crater, *Geophys.Res.Lett., 37*(4), L04201.

Morris, R., G. Klingelhöfer, C. Schröder, D. Rodionov, A. Yen, D. Ming, P. De Souza, I. Fleischer, T. Wdowiak, and R. Gellert (2006), Mössbauer mineralogy of rock, soil, and dust at Gusev crater, Mars: Spirit's journey through weakly altered olivine basalt on the plains and pervasively altered basalt in the Columbia Hills, *J. Geophys. Res, 111*.

Morris, R. V., D. W. Ming, R. Gellert, A. Yen, B. Clark, T. G. Graff, R. Arvidson, and S. Squyres (2008), The Hydrothermal System at Home Plate in Gusev Crater, Mars: Formation of High Silica Material by Acid-Sulfate Alteration of Basalt, *LPSC XXXIX, 1391*, 2208.

Murchie, S. L., et al (2009), A synthesis of Martian aqueous mineralogy after 1 Mars year of observations from the Mars Reconnaissance Orbiter, *J.Geophys.Res., 114*, E00D06.

Mustard, J. F., et al (2008), Hydrated silicate minerals on Mars observed by the Mars Reconnaissance Orbiter CRISM instrument, *Nature, 454*(7202), 305-309.

Nealson, K. H. (1997), The limits of life on Earth and searching for life on Mars, *J. Geophys. Res., 102*(E10), 23,675, doi: doi:10.1029/97JE01996.

Nisbet, E. G., and N. H. Sleep (2001), The habitat and nature of early life, *Nature, 409*(6823), 1083-1091.

Osterloo, M. M., V. E. Hamilton, J. L. Bandfield, T. D. Glotch, A. M. Baldridge, P. R. Christensen, L. L. Tornabene, and F. S. Anderson (2008), Chloride-Bearing Materials in

the Southern Highlands of Mars, *Science, 319*(5870), 1651-1654, doi: 10.1126/science.1150690.

Phelps, T., E. Murphy, S. Pfiffner, and D. White (1994), Comparison between geochemical and biological estimates of subsurface microbial activities, *Microb.Ecol., 28*(3), 335-349.

Pondrelli, M., A. Baliva, S. Di Lorenzo, L. Marinangeli, and A. P. Rossi (2005), Complex evolution of paleolacustrine systems on Mars: An example from the Holden crater, *J.Geophys.Res., 110*(E4), E04016.

Pondrelli, M., A. P. Rossi, L. Marinangeli, E. Hauber, K. Gwinner, A. Baliva, and S. Di Lorenzo (2008), Evolution and depositional environments of the Eberswalde fan delta, Mars, *Icarus, 197*(2), 429-451, doi: DOI: 10.1016/j.icarus.2008.05.018.

Poulet, F., J. P. Bibring, J. F. Mustard, A. Gendrin, N. Mangold, Y. Langevin, R. E. Arvidson, B. Gondet, and C. Gomez (2005), Phyllosilicates on Mars and implications for early martian climate, *438*(7068), 627.

Rothschild, L. J., and R. L. Mancinelli (2001), Life in extreme environments, *Nature, 409*(6823), 1092-1101.

Schink, B. (1997), Energetics of syntrophic cooperation in methanogenic degradation, *Microbiol.Mol.Biol.Rev., 61*(2), 262-280.

Schink, B. & Stams, A. J. M. (2002), Syntrophism among prokaryotes. In *The Prokaryotes. An Evolving Electronic Resource for the Microbiological Community*, release 3.8. Edited by M. Dworkin, K. H. Schleifer & E. Stackebrandt. New York: Springer.

Schulte, M., D. Blake, T. Hoehler, and T. McCollom (2006), Serpentinization and its implications for life on the early Earth and Mars, *Astrobiology, 6*(2), 364-376.

Shock, E.L. (1997), High-temperature life without photosynthesis as a model fro Mars, *JGR, 102*, 23,687-94.

Shock, E. L. (2009), Minerals as Energy Sources for Microorganisms, *Economic Geology, 104*(8), 1235-1248, doi: 10.2113/gsecongeo.104.8.1235.

Spear, J.R., J.J. Walker, T. McCollom and N.R. Pace (2005), Hydrogen and Bioenergetics in the Yellowstone Geothermal Ecosystem, *PNAS 102*(7): 2555-2560.

Squyres, S. W., J. P. Grotzinger, R. E. Arvidson, J. F. Bell, W. Calvin, P. R. Christensen, B. C. Clark, J. A. Crisp, W. H. Farrand, K. E. Herkenhoff, J. R. Johnson, G. Klingelhofer, A. H. Knoll, S. M. McLennan, H. Y. McSween, R. V. Morris, J. W. Rice, R. Rieder, and L. A. Soderblom (2004), In situ evidence for an ancient aqueous environment at Meridiani Planum, Mars, *Science, 306*(5702), 1709-1714.

Squyres, S. W., A. H. Knoll, R. E. Arvidson, B. C. Clark, J. P. Grotzinger, B. L. Jolliff, S. M. McLennan, N. Tosca, J. F. Bell III, W. M. Calvin, W. H. Farrand, T. D. Glotch, M. P. Golombek, K. E. Herkenhoff, J. R. Johnson, G. Klingelhofer, H. Y. McSween, and A. S. Yen (2006), Two years at Meridiani Planum: Results from the Opportunity Rover, *Science, 313*(5792), 1403-1407, doi: 10.1126/science.1130890.

Squyres, S., R. Arvidson, S. Ruff, R. Gellert, R. Morris, D. Ming, L. Crumpler, J. Farmer, D. Marais, and A. Yen (2008), Detection of Silica-Rich Deposits on Mars, *Science, 320*(5879), 1063.

Squyres, S. W., and A. H. Knoll (2005), Sedimentary rocks at Meridiani Planum: Origin, diagenesis, and implications for life on Mars, *EPSL, 240*(1), 1-10.

Stevens, T. O., and J. P. McKinley (1995), Lithoautotrophic microbial ecosystems in deep basalt aquifers, *Science, 270*(5235), 450-455, doi: 10.1126/science.270.5235.450.

Stevens, T. O., and J. P. McKinley (2000), Abiotic controls on H 2 production from basalt-water reactions and implications for aquifer biogeochemistry, *Environ.Sci.Technol., 34*, 826-831.

Treiman, A. H., J. D. Gleason, and D. D. Bogard (2000), The SNC meteorites are from Mars, *Planet.Space Sci., 48*(12-14), 1213-1230.

Varnes, E. S., B. M. Jakosky, and T. M. McCollom (2003), Biological potential of martian hydrothermal systems, *Astrobiology, 3*(2), 407-414.

Wray, J. J., B. L. Ehlmann, S. W. Squyres, J. F. Mustard, and R. L. Kirk (2008), Compositional stratigraphy of clay-bearing layered deposits at Mawrth Vallis, Mars, *Geophys.Res.Lett., 35*(12), L12202.

Yen, A., R. Morris, B. Clark, R. Gellert, A. Knudson, S. Squyres, D. Mittlefehldt, D. Ming, R. Arvidson, and T. McCoy (2008), Hydrothermal processes at Gusev Crater: An evaluation of Paso Robles class soils, *J.Geophys.Res, 113, E06S10, doi:10.1029/2007JE002978.*.

Zolotov, M. Y., and E. L. Shock (2005), Formation of jarosite-bearing deposits through aqueous oxidation of pyrite at Meridiani Planum, Mars, *Geophys.Res.Lett., 32*(21), L21203.